THE JOURNAL OF BIOLOGICAL CHEMISTRY Vol. 280, No. 8, Issue of February 25, pp. 6969–6985, 2005

Printed in U.S.A.

Galectin-1 Sensitizes Resting Human T Lymphocytes to Fas (CD95)-mediated Cell Death via Mitochondrial Hyperpolarization, Budding, and Fission*

Received for publication, August 25, 2004, and in revised form, November 3, 2004
Published, JBC Papers in Press, November 19, 2004, DOI 10.1074/jbc.M409752200

Paola Matarrese‡, Antonella Tinari§, Elisabetta Mormone‡, Germán A. Bianco¶, Marta A. Toscano¶, Barbara Ascione‡, Gabriel A. Rabinovich¶‖, and Walter Malorni‡‖‡‡**

From the Department of ‡Drug Research and Evaluation, and §Technology and Health, Istituto Superiore di Sanità, Viale Regina Elena, 299, Rome 00161, Italy and the ¶Laboratory of Inmunogenetics, Hospital de Clínicas José de San Martín, Faculty of Medicine, University of Buenos Aires, Avenida Córdoba 2351, 3er Piso, C1120 Buenos Aires, Argentina

Galectins have emerged as a novel family of immunoregulatory proteins implicated in T cell homeostasis. Recent studies showed that galectin-1 (Gal-1) plays a key role in tumor-immune escape by killing antitumor effector T cells. Here we found that Gal-1 sensitizes human resting T cells to Fas (CD95)/caspase-8-mediated cell death. Furthermore, this protein triggers an apoptotic program involving an increase of mitochondrial membrane potential and participation of the ceramide pathway. In addition, Gal-1 induces mitochondrial coalescence, budding, and fission accompanied by an increase and/or redistribution of fission-associated molecules h-Fis and DRP-1. Importantly, these changes are detected in both resting and activated human T cells, suggesting that Gal-1-induced cell death might become an excellent model to analyze the morphogenetic changes of mitochondria during the execution of cell death. This is the first association among Gal-1, Fas/Fas ligand-mediated cell death, and the mitochondrial pathway, providing a rational basis for the immunoregulatory properties of Gal-1 in experimental models of chronic inflammation and cancer.

Galectins, a growing family of carbohydrate-binding proteins, have recently attracted considerable attention as novel regulators of immune cell homeostasis (1–3). Despite extensive sequence homology and similar carbohydrate specificity, various members of this protein family behave as amplifiers of inflammatory response, whereas others activate homeostatic signals that serve to shut off immune effector functions (1–3). Recently, it has become clear that galectin-1 (Gal-1),[1] a member of this protein family, has the potential to impair T cell effector functions by antagonizing T cell activation (4), promoting growth arrest (5), and/or blocking proinflammatory cytokine secretion (6–8). Moreover, Gal-1 presented by the extracellular matrix promotes apoptosis of activated T cells in a carbohydrate-dependent manner, thus contributing to the establishment of immune cell tolerance (9–11). Interestingly, susceptibility to Gal-1-induced apoptosis is modulated by the regulated expression of specific glycosyltransferases (12, 13). Therapeutic administration of recombinant Gal-1 or its genetic delivery suppresses chronic inflammatory disorders by modulating T cell apoptosis *in vivo* (6, 8). In addition, we have recently demonstrated that Gal-1 contributes to the immune privilege of tumors by killing anti-tumor $CD4^+$ and $CD8^+$ effector T lymphocytes (14).

Freshly isolated T lymphocytes represent a physiological model system for the study of apoptosis in view of at least two clear cut features: (i) resting lymphocytes are generally resistant to various apoptotic stimuli including CD95/Fas ligation (15); (ii) T cell activation, *e.g.* via phytohemagglutinin (PHA) and/or interleukin-2 (IL-2) stimulation, leads to an increased susceptibility to cell death in a process called activation-induced cell death (16–18).

As a general rule, two different apoptotic pathways leading to the activation of cell-specific programs have been proposed: the "death receptor" and the "mitochondrial" pathways, involving caspase-8 and caspase-9, respectively (19). Both of them, however, involve significant morphogenetic changes of mitochondria (20) as well as changes of mitochondrial membrane potential (MMP), opening of the so-called mitochondrial megapore, and release of apoptogenic factors (21). However, there is still scarce information regarding the mechanisms underlying susceptibility of resting or activated T cells to physiological or pathological apoptotic stimuli.

In the present work we investigated the mechanisms underlying the proapoptotic activity exerted by Gal-1 in a physiological cell system represented by resting as well as activated human T cells. We found that this endogenous lectin can sensitize resting T cells and bolster activated T cells to Fas-mediated "physiological" cell death. The subcellular mechanism underlying these effects involves glycosphingolipid-mediated budding and fission of the mitochondria.

This is the first demonstration showing that Gal-1 sensitizes

* This work was supported by grants from the Ministry of Health and National Research Council (to W. M.) and by grants from Wellcome Trust, Antorchas Foundation, Sales Foundation, Ministry of Health (Carrillo-Oñativia Fellowship), and University of Buenos Aires Grant UBACYT M091 (to G. A. R.). The costs of publication of this article were defrayed in part by the payment of page charges. This article must therefore be hereby marked "*advertisement*" in accordance with 18 U.S.C. Section 1734 solely to indicate this fact.

‖ These authors contributed equally to this work.
** Member of CONICET (Consejo Nacional de Investigaciones Científicas y Tecnológias).
‡‡ To whom correspondence should be addressed: Dept. of Drug Research and Evaluation, Section of Cell Aging and Degeneration, Istituto Superiore di Sanitá, Viale Regina Elena 299, Rome 00161, Italy. Tel.: 39-06-4990-2905; Fax: 39-06-4990-3691; E-mail: malorni@iss.it.

[1] The abbreviations used are: Gal, galectin; Cyt *c*, cytochrome *c*; endo G, endonuclease G; FB_1, fumonisine B_1; FITC, fluorescein isothiocyanate; HD, healthy donor; IL-2, interleukin-2; IVM, intensified video microscopy; JC-1, 5–5′,6–6′-tetrachloro-1,1′,3,3′-tetraethylbenzimidazol-carbocyanine iodide; mAb, monoclonal antibody; MMP, mitochondrial membrane potential; Mon, monensin; PHA, phytohemagglutinin; PI, propidium iodide; *p*NA, *p*-nitroanilide; TEM, transmission electron microscopy; TRITC, tetramethylrhodamine isothiocyanate; UCP-2, uncoupler protein 2.

resting human T cells to undergo apoptosis. Elucidation of the cellular and molecular mechanisms involved in Gal-1 effects is essential for a complete understanding of the immunosuppressive effects of this protein and its novel role in tumor-immune privilege (14). This study also demonstrates that a dynamic imbalance of mitochondrial fusion/fission processes can effectively be involved in apoptosis of nonengineered freshly isolated primary cells.

EXPERIMENTAL PROCEDURES

Isolation and Activation of Peripheral Blood Lymphocytes—Human peripheral blood lymphocytes from healthy donors (HDs) were isolated from freshly heparinized blood through a Ficoll-Hypaque density gradient centrifugation and washed three times in phosphate-buffered saline, pH 7.4 (Lympholyte-H, Cedarlane Laboratories, Hornby, Ontario, Canada). Peripheral blood lymphocytes were subcultured in 25-cm^2 or 75-cm^2 Falcon plastic flasks at a density of $\sim 1 \times 10^6$ cells/ml in RPMI 1640 (Invitrogen) containing 15% fetal calf serum (Flow Laboratories, Irvine, Scotland, UK), 1% nonessential amino acids, 5 mM L-glutamine, 100 IU/ml penicillin, and 100 mg/ml streptomycin at 37 °C in a humidified 5% CO_2 atmosphere. For peripheral blood lymphocyte activation, $CD3^+$ T cells purified by magnetic beads (Dynal, Great Neck, NY) were cultured for 72 h with 2 μg/ml PHA (Roche Applied Science) and 60 IU/ml IL-2 (Invitrogen).

Biochemical Characterization of Human Recombinant Gal-1—Human recombinant Gal-1 was obtained and purified as described by Hirabayashi *et al.* (22). In brief, *Escherichia coli* strain BL21 (DE3) (Novagen) was transformed with the pET21a/hGal1 plasmid (kindly provided by Drs. Hirabayashi and K. I. Kasai), and human Gal-1 expression was assessed by immunoblotting. The recombinant protein was purified by affinity chromatography on an asialofetuin-agarose column and eluted with lactose after extensive washing of the column. The hemagglutinating activity was measured as described previously (10, 22), and the NH_2-terminal amino acid sequence was determined with an Applied Biosystems model 477A pulsed liquid sequencer (Applied Biosystems, Inc.). The lipopolysaccharide content of the purified sample was less than 60 ng/mg protein, determined by a colorimetric endotoxin determination reagent (Pyrodick, Seikagaku, Tokyo). The eluted protein was reactive with an anti-Gal-1-specific polyclonal rabbit antibody, and the minimum concentration of protein required for hemagglutinating activity was ~ 1 μg/ml (10, 22). The concentration-dependent monomer/dimer status of Gal-1, assessed by nonreducing PAGE and immunoblotting, is documented in Fig. 1*A*.

In Vitro Treatments—Previous to cell death, binding of Gal-1 to human resting and activated T cells was performed using biotinylated Gal-1 and FITC-streptavidin in the absence or presence of 30 mM lactose as described previously (9). Isolated human T cells (resting or PHA/IL-2-activated) were treated with different concentrations of Gal-1 (5, 20, 50, and 100 μg/ml) for different time periods (6, 18, 36, and 72 h) in association, or not, with 500 ng/ml anti-human Fas IgM mAb (α-Fas, clone CH11, Upstate Biotechnology, Lake Placid, NY). As a negative experimental control an equal concentration of anti-CD3 IgM was also employed. Gal-1 and CH11 treatments were also performed: (i) in the presence of neutralizing anti-human Fas IgG1 mAb (clone ZB4, Upstate Biotechnology, 250 ng/ml); (ii) in cells pretreated for 1 h with 5 μM ZVAD-CHO (a pan-caspase inhibitor, R&D Systems, Minneapolis); or (iii) in cells incubated in the presence of 30 mM lactose. To evaluate the involvement of ceramide-mediated signaling in Gal-1-induced apoptosis, resting lymphocytes were pretreated for 1 h with a combination of specific inhibitors of the ceramide pathway: 20 μM fumonisine B_1 (B_1; Sigma) and 10 μM monensin (Mon; Sigma) (both solubilized in dimethyl sulfoxide) before the addition of Gal-1. Although FB_1 inhibits sphingolipid and glycosphingolipid synthesis via (dihydro)ceramide synthesis inhibition (23), Mon prevents ceramide generation through inhibition of acidic sphingomyelinase (24). Dimethyl sulfoxide given alone was used as an additional control.

Evaluation of Cell Surface Receptors—The surface expression of molecules associated with T cell activation (CD69, CD38, and HLA-DR) and cell death (CD95/Fas) was assessed by flow cytometry on resting and activated T lymphocytes treated with Gal-1. For this purpose, we used fluorochrome-conjugated FITC or mAbs raised against human CD95, CD38, HLA-DR and CD69 (BD Biosciences). Appropriate fluorochrome-conjugated mAbs of the same isotype were used as negative controls.

Cell Death Assays—Quantitative evaluation of apoptosis was performed by using the following flow and static cytometry methods: (i) double staining using FITC-conjugated annexin V/propidium iodide (PI) apoptosis detection kit (Eppendorf, Milan, Italy); (ii) staining with chromatin dye Hoechst (Molecular Probes, Eugene, OR), as described previously (25); and (iii) evaluation of DNA fragmentation in ethanol-fixed cells using PI (Sigma) (data not shown). To rule out the possibility that Gal-1-induced cell agglutination may damage the cells, we incubated the cells with 30 mM lactose to dissociate cell clusters after Gal-1 binding and before cell death assays.

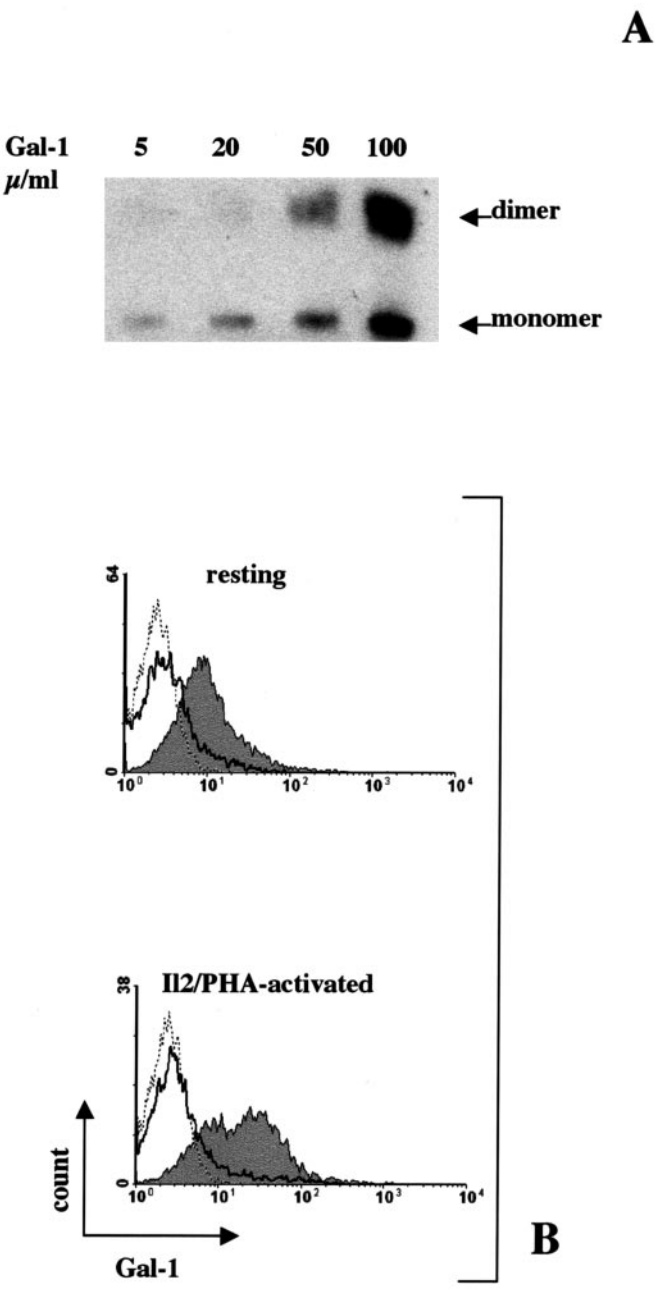

FIG. 1. **Biochemical and functional characterization of human recombinant Gal-1.** *A*, monomer-dimer status of purified recombinant Gal-1 at concentrations ranging from 5 to 100 μg/ml used for functional assays. Samples were run on a 15% nondenaturing polyacrylamide gel, transferred onto nitrocellulose membranes, and incubated with a specific rabbit anti-Gal-1 polyclonal Ab. *B*, for binding assays 5×10^5 PHA/IL-2-activated or resting T cells were incubated for 1 h with 20 μg/ml biotinylated Gal-1 in the absence (*gray histograms*) or presence (*black empty histograms*) of 30 mM lactose. Cells were then incubated with FITC-streptavidin for 45 min and analyzed by flow cytometry.

Analysis of the MMP—The MMP of control and treated cells was studied by using the JC-1 probe. Briefly, cells were stained with 10 μM JC-1 (Molecular Probes) as described previously (26). Tetramethylrhodamine ester (1 μM, TMRM, Molecular Probes, red fluorescence) was also used to confirm the data obtained using JC-1.

Cell Cycle Analyses—For DNA analysis ethanol-fixed lymphocytes

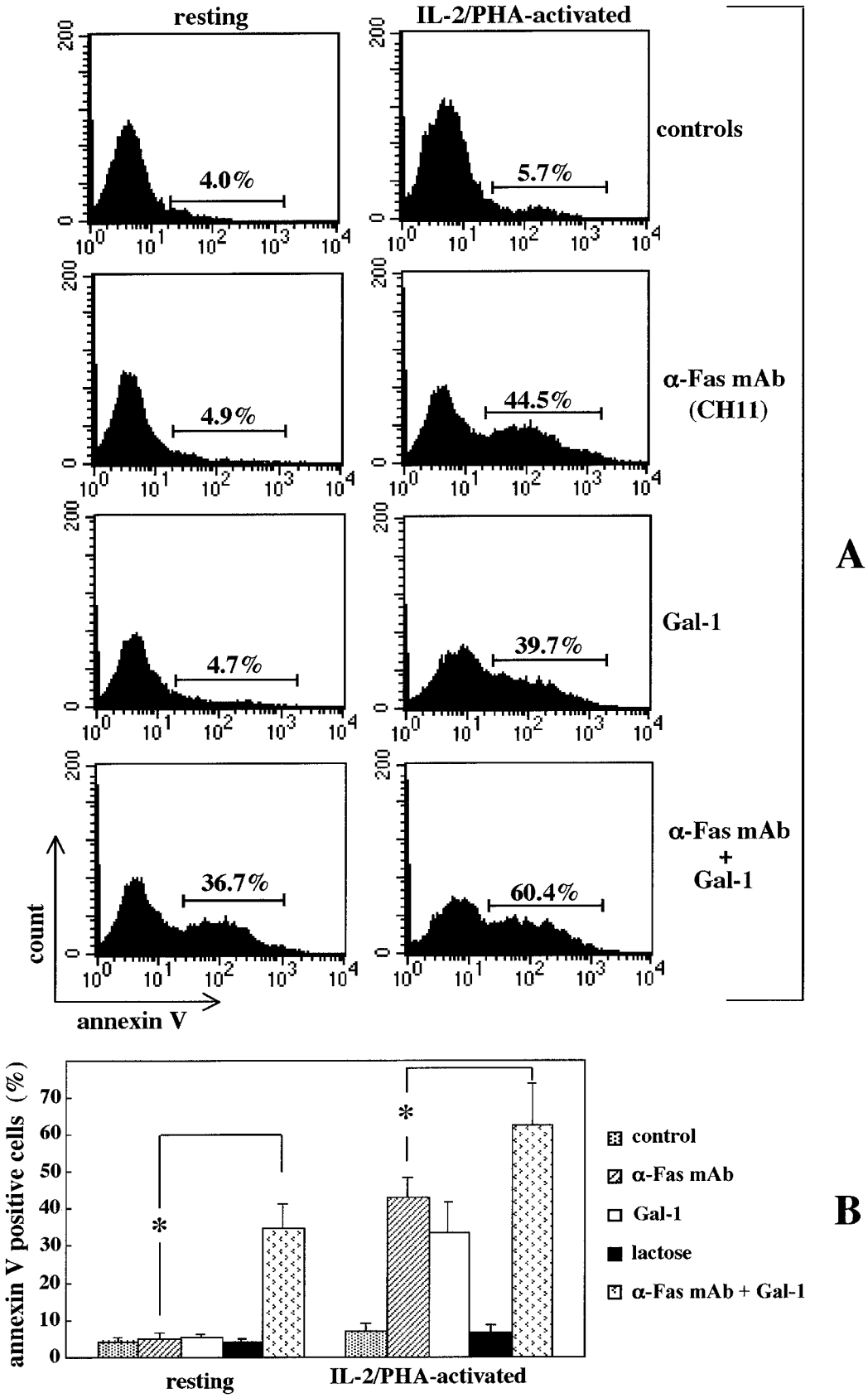

FIG. 2. **Gal-1 sensitizes resting and activated T lymphocytes to Fas-mediated cell death.** *A*, percentage of apoptosis as revealed by flow cytometry analysis of resting and PHA/IL-2-activated freshly isolated human T lymphocytes after annexin V-FITC staining. The *first row* includes controls; the *second row* shows apoptosis induced by α-Fas triggering (CH11); the *third row* indicates resting and activated cells cultured with 20 μg/ml Gal-1 in the absence of other stimuli; the *fourth row* indicates association of CH11 and Gal-1. Results obtained from a representative HD are shown. *Numbers* indicate the percentage of annexin V-positive cells. Similar results were obtained by the analysis of hypodiploid peaks after PI staining (not shown). *B*, mean values ± S.D. obtained by pooling together data from 12 different HDs. *Asterisks* (*) represent $p < 0.01$. Note that the presence of 30 mM lactose significantly prevented Gal-1 effects.

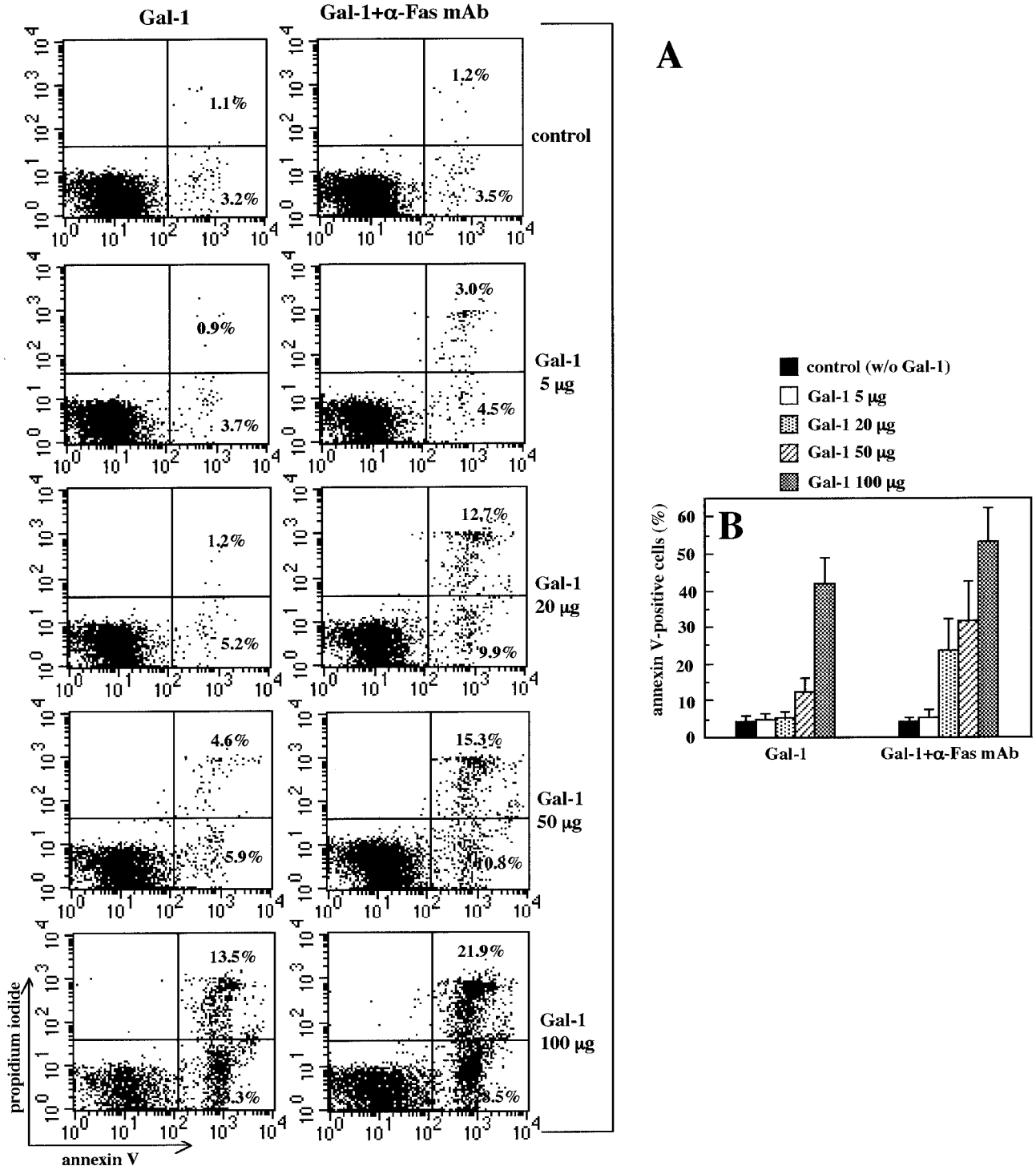

FIG. 3. **Gal-1 sensitizes resting T cells to Fas-mediated apoptosis in a dose-dependent manner.** *A*, biparametric flow cytometry analysis of resting lymphocytes after double staining with annexin V-FITC/PI. *A*, *left column*, T lymphocytes treated with increasing doses of recombinant human Gal-1; *right column*, T cells treated with Gal-1 + CH11 combination. In the *upper* and *lower right quadrants* of each plot, annexin V/PI double positive cells and annexin V single positive cells are represented, respectively. Results obtained from a representative HD are reported. *B*, mean values ± S.D. of the percentages of annexin V-positive cells obtained by evaluating cells from 12 different HDs. Statistical analyses indicated that (i) 50 and 100 μg/ml Gal-1 exposure induced *per se* annexin V staining of human resting T lymphocytes and that (ii) Gal-1 significantly bolstered anti-Fas-induced cell death ($p < 0.01$).

were incubated with μg/ml PI (Sigma) and 10 μM RNase (Sigma) for 45 min. After this time period, samples were acquired directly on a FACScan flow cytometer by CellQuest software (BD Biosciences). At least 20,000 events for each sample were statistically analyzed by ModFIT software for Macintosh to determine the percentage of cells in G_0/G_1, S, and G_2/M phases, respectively.

Analysis of the Redox Balance—Resting and PHA/IL-2-activated human T lymphocytes (5×10^5 cells), cultured in the presence or absence of Gal-1, were incubated in 495 μl of Hanks' balanced salt solution (pH 7.4) containing 10 μM dihydrorhodamine 123 (Molecular Probes) or 1 μM dihydroethidium (Molecular Probes) in polypropylene test tubes for 15 min at 37 °C. Intracellular content of reduced thiols was explored by using 10 μM 5-chloromethyl-2′,7′-dichloro-dihydrofluoresceindiacetate (Molecular Probes). Cells exposed to the GSH depleting drug L-buthionine-[*S*,*R*]-sulfoximine (7.5 mM; Sigma) for 16 h were considered as negative controls (data not shown). The median values of fluorescence

intensity histograms were used to provide semiquantitative assessment of reduced thiols content and reactive oxygen intermediates production.

Analysis of Caspase Activation—For detection of the active form of caspases-8, -9, and -3, colorimetric protease assay kits (Chemicon International, Inc.) were used. Proteins obtained from cytosolic extracts (50–200 μg) were incubated with 200 μM IETD-*p*NA (for caspase-8), LEHD-*p*NA (for caspase-9) or DEVD-*p*NA (for caspase-3). The assay was based on the spectrophotometric detection of the chromophore *p*-nitroanilide (*p*NA) after cleavage from the labeled substrates. *p*-NA light emission was quantified using a microtiter plate reader at 405 nm. Comparison of the absorbance of *p*-NA from apoptotic samples with nonstimulated controls allowed determination of the-fold increase in caspase activity (27).

Immunocytochemistry—Immunofluorescence analyses were performed by double staining as follows. Briefly, control and treated samples were incubated, with 1 μM Mito Tracker Green FM (Molecular Probes) at 37 °C for 30 min. Then, cells were washed, fixed with 4% paraformaldehyde (w/v in phosphate-buffered saline) for 1 h at room temperature, and then permeabilized by 0.5% (v/v) Triton X-100. For localization and quantification of h-Fis, DRP-1 and uncoupler (UCP) proteins, samples were incubated for 1 h at room temperature with mAbs specific to h-Fis (Alexis Biochemicals, San Diego), DRP-1 (BD Biosciences), or UCP-2 (Calbiochem). Negative controls were incubated with normal mouse serum. After several washings, samples and isotype controls were incubated for 45 min at room temperature with TRITC-conjugated anti-mouse IgG (Sigma). All samples were mounted with glycerol phosphate-buffered saline (2:1) and analyzed by Intensified Video Microscopy (IVM) as stated elsewhere (28) or analyzed by flow cytometry.

Analysis of Fas Ligand Secretion—Fas ligand levels were determined in supernatants of lymphocytes cultured in the presence or absence of Gal-1, using a sensitive enzyme-linked immunosorbent assay kit (R&D). Briefly, resting and PHA/IL-2-activated lymphocytes were exposed to Gal-1 for different time periods. Supernatant aliquots were removed 6, 18, 36, and 72 h after exposure to Gal-1 and assayed for Fas ligand secretion according to the manufacturer's instructions.

Analysis of Cytochrome c Release—Cytochrome *c* (Cyt *c*) was evaluated by a sensitive and specific immunoassay, using a commercial enzyme-linked immunosorbent assay kit according to the manufacturer's instructions. The light emitted was quantified by using a microtiter plate reader at 405 nm. Cyt *c* concentration was expressed as μg/ml.

Transmission Electron Microscopy (TEM)—For TEM examination, cells were fixed in 2.5% cacodylate-buffered (0.2 M, pH 7.2) glutaraldehyde for 20 min at room temperature and postfixed in 1% OsO_4 in cacodylate buffer for 1 h at room temperature. Fixed specimens were dehydrated through a graded series of ethanol solutions and embedded in Agar 100 (Agar Aids, Cambridge, UK). Serial ultrathin sections were collected on 200-mesh grids and then counterstained with uranyl acetate and lead citrate. Sections were observed with a Philips 208 electron microscope at 80 kV.

Morphometric Analyses—Analyses of mitochondrial intracellular localization were carried out by TEM observation of at least 200 cells at the same magnification (3,000×). Values were expressed as the percentage of cells displaying clusters of mitochondria at one pole of the cells with respect to lymphocytes with randomly distributed mitochondria.

Immunoelectron Microscopy—Thin sections, collected on gold grids, were treated with phosphate-buffered saline containing 1% (w/v) gelatin, 1% bovine serum albumin, 5% fetal calf serum, and 0.05% Tween 20 and then incubated with mAbs raised against anti-Cyt *c*, endonuclease G (endo G), DRP-1, and h-Fis diluted 1:10 in the same buffer without gelatin overnight at 4 °C. After washing for 1 h at room temperature, sections were labeled with a protein A-10 nm gold conjugate (1:10) for 1 h at room temperature and washed again. Negative controls were incubated with the gold conjugate alone.

Data Analysis and Statistics—All samples were analyzed with a FACScan cytometer (BD Biosciences) equipped with a 488 argon laser. At least 20,000 events were acquired. Data were recorded and analyzed statistically by a Macintosh computer using CellQuest Software. The expression level of the analyzed proteins was expressed as a median value of the fluorescence emission curve, and the statistical significance was calculated by using the parametric Kolmogorov-Smirnov test. Statistical analyses of apoptosis data were performed by using Student's *t* test or one-way analysis of variance using the Statview program for Macintosh. All data reported were verified in 12 different HDs and are expressed as the mean ± S.D. Only *p* values of less than 0.01 were considered as statistically significant.

TABLE I

Effects of Gal-1 on the expression of activation markers

Flow cytometry analysis of surface expression of CD69, HLA-DR, and CD38 in resting and IL-2/PHA-activated T cells after 20 μg/ml Gal-1 treatment for 72 h is shown. Numbers represent the mean ± S.D. of the median values of the fluorescence intensity histograms from four different experiments.

	Resting		PHA/IL-2-activated	
	Control	Gal-1	Control	Gal-1
CD69	1.9 ± 0.5	1.7 ± 0.4	15.9 ± 3.1	14.9 ± 1.9
HLA-DR	47.8 ± 7.9	50.1 ± 6.3	385.4 ± 23.1	383.9 ± 22.5
CD38	15.2 ± 2.2	15.9 ± 1.7	83.5 ± 10.0	82.9 ± 9.1

RESULTS

Gal-1 Sensitizes Resting T Cells to Anti-Fas (α-Fas)-mediated Apoptosis in a Dose-dependent Manner—The first set of experiments was carried out to evaluate the ability of recombinant Gal-1 to modulate the susceptibility of human freshly isolated T cells, both resting and PHA/IL-2-activated, to Fas (CD95)-mediated apoptosis. Recombinant human Gal-1 was obtained, purified, and characterized, as described under "Experimental Procedures" (see also Fig. 1*)*. The lipopolysaccharide content of the purified protein was less than 60 ng/mg protein as has been described previously (22). Before the cell death assays we analyzed binding of biotinylated Gal-1 to human resting and activated T cells. Biotinylated Gal-1 (20 μg/ml) bound with higher affinity to PHA/IL-2-activated, compared with resting human T cells (Fig. 1*B*; *gray histograms*). Gal-1 binding to activated and resting T cells was inhibited completely in the presence of 30 mM lactose, demonstrating that binding was specific and saccharide-dependent (Fig. 1*B*, *black empty histograms*).

We observed that Gal-1, at a concentration of 20 μg/ml, was capable of inducing a time-dependent phosphatidylserine exposure and annexin V binding in a significant percentage of activated T cells. In particular, the percentages of annexin V-positive cells were 7.9% ± 2.3% after 6 h, 12.3% ± 3.0% after 18 h, and 22.1% ± 4.9% after 36 h. Results obtained after 72 h of Gal-1 exposure are reported in Fig. 2*A* (a representative HD, *third row*, *right panel*) and Fig. 2*B* (mean values from 12 different HDs). By contrast, the same Gal-1 concentration was ineffective toward resting T lymphocytes (Fig. 2*A*, *third row*, *left panel*). Importantly, the presence of 30 mM lactose completely inhibited Gal-1-induced phosphatidylserine exposure in both resting and activated lymphocytes (Fig. 2*B*). Control experiments carried out using the anti-Fas mAb (clone CH11) clearly pointed out the powerful proapoptotic activity elicited by Fas ligation on activated cells, *i.e.* the so-called activation-induced cell death (17) (Fig. 2*A*, *second row*, *right panel*). Interestingly, exposure to 20 μg of Gal-1 significantly sensitized resting lymphocytes to anti-Fas apoptotic triggering inducing higher apoptotic rates (36.7%) compared with control samples (Fig. 2*A*, *bottom row*, *left panel*, Δ% Gal-1 + CH11 *versus* CH11 alone = 86.6%). In the same vein, in activated T cells, Gal-1 treatment further increased the effects induced by CD95 engagement, significantly bolstering apoptosis (60.4%, Fig. 2*A*, *bottom row*, *right panel*). Results obtained by pooling together data from blood samples of 12 different HDs are reported in Fig. 2*B*.

A dose-dependent response could be observed when human T cells were exposed to increasing concentrations of Gal-1 (Fig. 3*A*). In particular, doses of Gal-1 ranging from 20 to 100 μg/ml induced a significant ($p < 0.01$) sensitization to anti-Fas apoptotic triggering (Fig. 3*A*, a representative HD, compare *right panel* with *left panel*, *upper* and *lower right quadrants*). Strikingly, considering the general resistance of resting T cells to apoptosis (15, 16), we have noticed that a relatively high con-

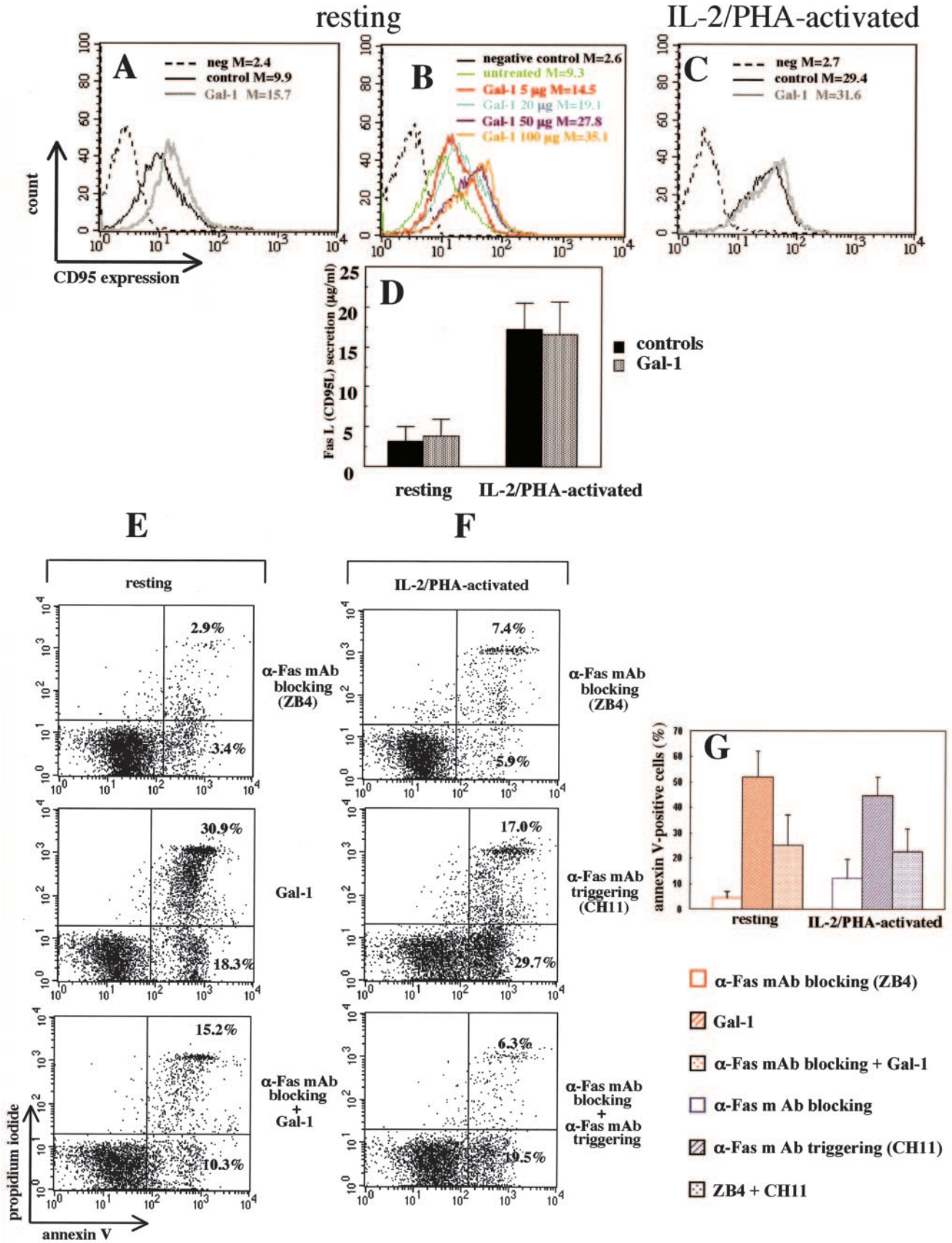

FIG. 4. **Association of Fas and Gal-1 in the execution of T cell death.** Flow cytometry analysis of CD95 surface expression in (*A*) resting T cells and (*C*) PHA/IL-2-activated T lymphocytes is shown. Note that the presence of 20 µg/ml Gal-1 significantly increased CD95 expression in resting cells but not in activated cells. *B*, flow cytometry evaluation of CD95/Fas surface expression in resting lymphocytes treated with increasing concentrations of Gal-1. *Numbers* represent median values of fluorescence intensity histograms (*M*) obtained from a representative HD. *D*, analysis of Fas ligand secretion by a capture enzyme-linked immunosorbent assay. Data from six different HDs are reported. No significant changes were detectable in resting or activated T cells after Gal-1 treatment compared with controls. *E–G*, biparametric flow cytometry analysis after double

TABLE II
Influence of Gal-1 on the redox state of human T cells

Semiquantitative cytofluorometric analysis of hydrogen peroxide production, superoxide anion production, and intracellular reduced thiols content in resting and activated T lymphocytes after different treatments (20 μg/ml, 72 h) are shown. Numbers represent the mean ± S.D. of the median values of the fluorescence intensity histograms from four different experiments.

	Resting				Activated			
	Control	Gal-1	α-Fas	Gal-1 + α-Fas	Control	Gal-1	α-Fas	Gal-1 + α-Fas
H_2O_2	82.8 ± 9	79.7 ± 8	79.1 ± 7	106.9 ± 11	115.5 ± 10	160.9 ± 12	100.3 ± 9	174.8 ± 17
O_2	63.8 ± 7	66.7 ± 9	64.4 ± 6	65.4 ± 6	73.6 ± 8	74.3 ± 8	77.7 ± 6	76.9 ± 9
Thiols	210.9 ± 23	229.7 ± 19	234.8 ± 25	279.8 ± 29	399.5 ± 31	491.4 ± 39	454.2 ± 34	499.4 ± 41

centration of Gal-1 (100 μg) (6, 8) was *per se* a powerful apoptotic inducer in human resting T cells (Fig. 3*A*, *last row*, representative HD). Mean values obtained by pooling together median values from 12 different HDs are reported in Fig. 3*B*.

Subcellular Effects Triggered by Gal-1 on Resting and Activated T Cells—In light of the above findings, we next evaluated the expression of relevant cell surface markers and cellular mediators associated with cell activation and cell fate in resting and activated lymphocytes after exposure to Gal-1. Our attention was essentially focused on: (i) cell activation markers, (ii) CD95/Fas expression, and (iii) Fas ligand expression and secretion. Moreover, in consideration of the role of reactive oxygen intermediates in disturbing cell homeostasis and modulating cell apoptosis (29), we also explored the redox state of Gal-1-treated and untreated cells. Regarding activation markers, no changes could be detected after Gal-1 treatment in either resting or activated T cells. In particular, CD69, major histocompatibility complex class II, and CD38 remained unchanged in Gal-1-exposed cells compared with controls (Table I). Thus, Gal-1 was not able *per se* to modulate expression of T cell activation markers. In contrast, we observed a significant ($p < 0.01$) up-regulation of CD95/Fas expression on the surface of resting T lymphocytes exposed to Gal-1 (Fig. 4*A*; a representative HD is shown). Mean values obtained from median values of fluorescence intensity histograms in resting cells from 12 HD are as follows: control = 9.4 ± 1.5%: Gal-1 = 16.2 ± 2.4% ($p < 0.01$). Interestingly, we found a dose-dependent up-regulation of this molecule on the surface of resting cells treated with Gal-1 (Fig. 4*B*). By contrast, under our experimental conditions, PHA/IL-2-activated cells did not display significant changes in CD95/Fas surface expression after Gal-1 treatment (Fig. 4*C*). In fact, mean values obtained by pooling together median values of fluorescence intensity histograms in activated T lymphocytes from 12 HDs were the following: PHA/IL-2 = 30.3 ± 4.5; PHA/IL-2 + Gal-1 = 32.4 ± 5.1% ($p > 0.05$). The influence of Gal-1 on Fas ligand secretion was also evaluated under the same experimental conditions in the culture medium of treated and untreated cells. However, no significant changes were detected between control and Gal-1-treated lymphocytes, either in culture medium from resting or PHA/IL-2-activated T cells (Fig. 4*D*). Accordingly, when intracellular and surface expression of Fas ligand was evaluated, no significant changes were found after Gal-1 treatment (data not shown).

Next, a specific set of experiments was carried out to analyze three critical parameters known to influence the redox balance of the cell: (i) production of superoxide, (ii) hydrogen peroxide, and (iii) the intracellular content of reduced thiols. As shown in Table II, no significant changes were detected in the redox state of resting cells after treatment with both Gal-1 and anti-Fas mAb. In contrast, in PHA/IL-2-activated T cells, we found a significant increase in hydrogen peroxide production after Gal-1 treatment and a significant increase in thiol content in Gal-1 as well as in anti-Fas-treated cells (Table II shows median values of the fluorescence intensity histograms obtained by flow cytometry). Importantly, no significant changes were detected between Gal-1-treated and control cells in terms of cell proliferation and cell cycle (Table III).

TABLE III
Effects of Gal-1 on cell cycle and proliferation of human T cells

Cytofluorometric analysis of the cell cycle of resting and PHA/IL-2-activated T cells after 20 μg/ml Gal-1 treatment for 72 h is shown. Numbers represent the mean percentage ± S.D. of cells in G_0/G_1, S, and G_2/M phases from three independent experiments, respectively. Statistical analysis was performed by ModFIT software for Macintosh. Effects of Gal-1 treatment on cell proliferation are expressed as cell no./ml (bottom row).

	Resting		PHA/IL-2-activated	
	Control	Gal-1	Control	Gal-1
G_0/G_1 (% of cells)	92.9 ± 2.1	93.0 ± 1.9	78.7 ± 1.7	79.2 ± 2.0
S (% of cells)	2.7 ± 0.6	2.5 ± 0.5	11.3 ± 2.1	10.0 ± 2.2
G_2/M (% of cells)	4.4 ± 1.1	4.5 ± 1.0	10.0 ± 1.8	10.8 ± 1.9
Cell no. (× 10^5/ml)	6.7 ± 0.2	6.5 ± 0.7	7.6 ± 1.0	7.4 ± 1.3

On the basis of our findings, we next performed a set of experiments aimed at elucidating the association between Gal-1 and Fas-mediated apoptosis. For this purpose we used the anti-Fas-blocking mAb (clone ZB4) and analyzed the percentage of annexin V/PI-positive cells (Fig. 4*E*). As a control, we used the anti-Fas-blocking mAb ZB4 on PHA/IL-2-activated T lymphocytes treated with anti-Fas-triggering mAb (clone CH11) (Fig. 4*F*). As expected, ZB4 was able to counteract anti-Fas (CH11)-induced apoptosis significantly in activated T cells (Fig. 4*F*; a representative HD; compare the *middle panel* with the *bottom panel*). More importantly, we found that in the presence of the ZB4 blocking mAb, a significant reduction of Gal-1-induced cell death clearly occurred in resting cells (Fig. 4*E*, compare the *middle panel* with the *bottom panel*). The results obtained by pooling together data from 12 different HDs clearly indicated that CD95/Fas-blocking mAb ZB4 was able to prevent Gal-1-induced cell death significantly in resting cells (Δ = 50%; Fig. 4*G*).

Influence of Gal-1 on MMP of Resting Human T Lymphocytes—To deep inside the molecular mechanisms involved in Gal-1 sensitization to anti-Fas-induced cell death we analyzed MMP in resting cells sensitized to Fas triggering by exposure to Gal-1 (Fig. 5, *A–F*). We found an increased MMP in a signifi-

staining with annexin V-FITC/PI of (*E*) resting T lymphocytes treated with 100 μg/ml Gal-1 in the presence or absence of α-Fas blocking mAb (ZB4 clone). In *F*, PHA/IL-2-activated lymphocytes were treated with α-Fas-mAb (CH11) in the presence or absence of ZB4, a control, to evaluate the antagonistic activity of ZB4 mAb. In the *upper* and *lower right quadrants*, the percentages of annexin V/PI double positive cells and annexin V single positive cells are included, respectively. Results obtained from a representative HD are reported. *G*, mean values ± S.D. of the percentages of annexin V-positive cells obtained by evaluating cells from 12 different HDs. Statistical analyses indicate a significant ($p < 0.01$) inhibition of apoptosis by the ZB4 antagonist mAb in Gal-1-treated resting T lymphocytes (*red columns*). Note that ZB4 mAb treatment also prevented α-Fas-mAb (CH11)-induced apoptosis in PHA/IL-2-activated T lymphocytes (positive control, *blue columns*).

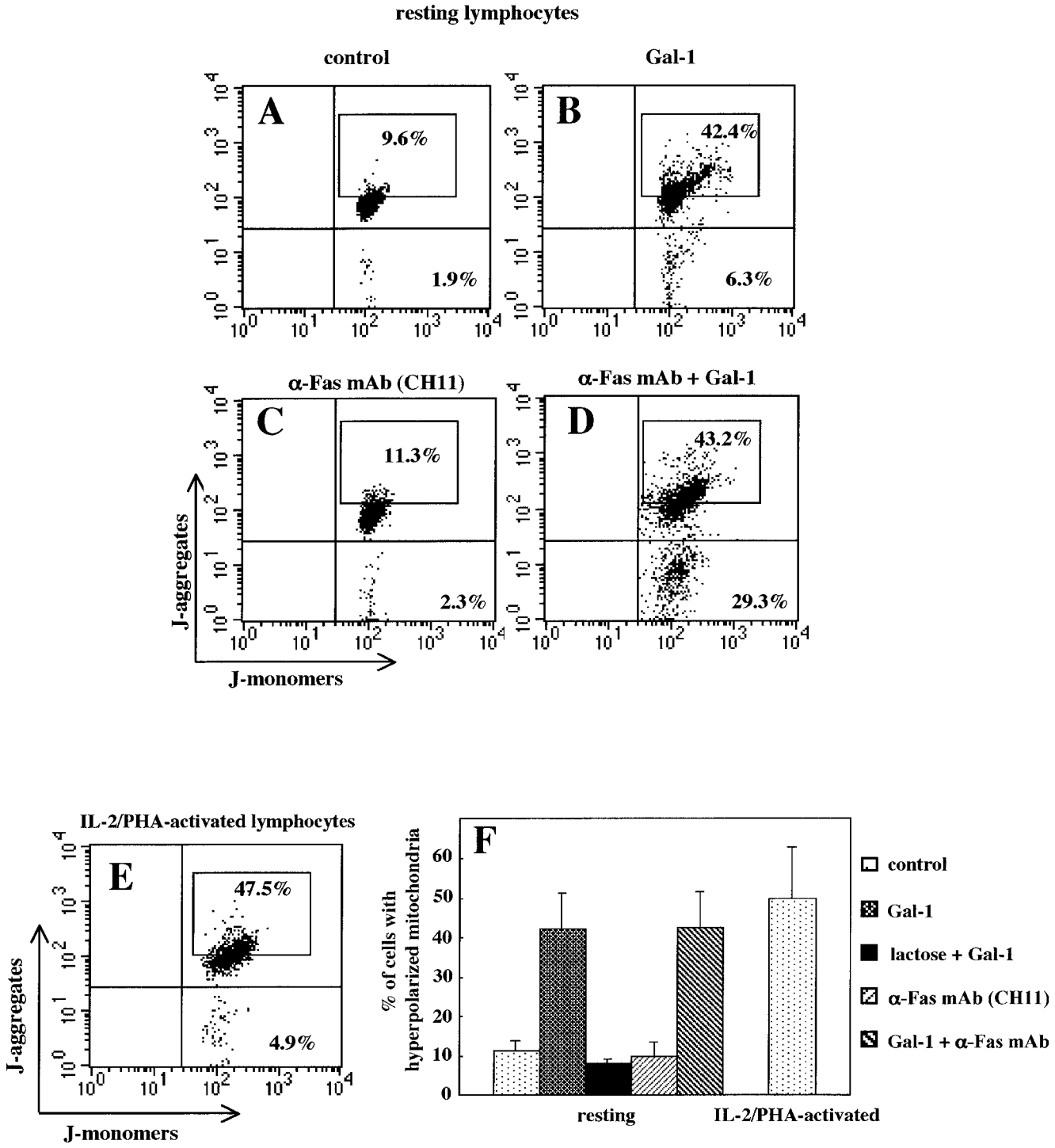

FIG. 5. **Modulation of MMP by Gal-1 in human resting T lymphocytes.** Biparametric flow cytometry analysis of MMP of resting T lymphocytes after staining with JC-1 (*A–D*). *A*, control; *B*, 20 μg/ml Gal-1; *C*, α-Fas mAb (CH11); and *D*, association of α-Fas mAb (CH11) and Gal-1. E, PHA/IL-2-activated T lymphocytes (positive control for mitochondrial membrane hyperpolarization). *Numbers* reported in the *boxed area* represent the percentages of cells with hyperpolarized mitochondria. In the *lower right quadrants* the percentages of cells with depolarized mitochondria are shown. In *A–E*, results obtained from a representative HD are shown. *F*, mean values ± S.D. of the percentages of cells with hyperpolarized mitochondria obtained by evaluating six different HDs. Statistical analyses indicated a significant ($p < 0.01$) increase of cells with hyperpolarized mitochondria in resting T lymphocytes treated with Gal-1 and the α-Fas mAb (CH11) and in PHA/IL-2-activated T lymphocytes (positive control) with respect to untreated resting cells. Note that the presence of 30 mM lactose significantly prevented mitochondrial membrane hyperpolarization.

cant percentage of Gal-1-treated resting T lymphocytes (Fig. 5*B*; the *boxed area* shows the percentage of cells with hyperpolarized mitochondria). By contrast, and according to apoptosis data (see Fig. 2): (i) anti-Fas mAb given alone (clone CH11) did not induce any significant change in MMP (Fig. 5*C*, *boxed area*) whereas (ii) Gal-1/CH11 association also induced in resting lymphocytes the loss of MMP in a significant percentage of cells, a typical afterward modification associated with apoptosis execution (Fig. 5*D*, *lower right quadrant*). Noteworthy, the association of Gal-1 with anti-Fas (CH11) left substantially unchanged the percentage of cells with hyperpolarized mitochondria with respect to cells treated with Gal-1 alone (Fig. 5*D*

versus Fig. 5B). As a positive control for this set of experiments, we used PHA/IL-2-activated lymphocytes, which show hyperpolarized mitochondria as a "default" feature, as reported previously (30–32) (Fig. 5*E*, *boxed area*). In summary, data obtained by analyzing T cells from 12 different HDs (reported as mean values in Fig. 5*F*) clearly indicate that: (i) when resting cells were exposed to Gal-1 or Gal-1 + CH11, an increased MMP was detectable (Gal-1 = 42.1 ± 8.1; Gal-1 + CH11 = 43.3 ± 9.4) and, importantly (ii) in these cells CH11 given alone did not influence MMP. Furthermore, these effects were almost completely prevented using β-galactoside-related sugars such as lactose (30 mM). In fact, lactose also inhibited the effects induced by Gal-1 at the mitochondrial level (Fig. 5*F*). A summary of the findings observed upon Gal-1 treatment of human lymphocytes is shown in Table IV.

Considering these observations, we next explored time-dependent changes in MMP on human resting T cells after Gal-1 treatment. As shown in Fig. 6, very early after Gal-1 treatment, an increased MMP, *i.e.* a *hyperpolarization* of mitochondrial membrane, was detected in a high percentage of cells (Fig. 6, *B* and *C*, 6 and 18 h, respectively, see *boxed area*) followed by a typical *depolarization*, as a later event (Fig. 6, *D* and *E*, 36 and 72 h, respectively, see the *lower right quadrant*). In these experiments, the release of Cyt *c* was also assessed (Fig. 6*F*). Importantly, the percentage of cells in which we observed the loss of MMP corresponded to the percentage of lymphocytes that showed surface exposure of phosphatidylserine as a typical feature of apoptosis (compare Fig. 6, *A–E*, with Fig. 7*A*).

TABLE IV
Effects of Gal-1 on human T cells

Changes induced by Gal-1 (20 μg/ml, 72 h) in resting and IL-2/PHA-activated T lymphocytes are shown.

	Resting	IL-2/PHA-activated
Fas-mediated apoptosis	Increased	Increased
Gal-1-induced apoptosis	No changes	Increased
CD95 expression	Increased	No changes
Fas ligand secretion	No changes	No changes
Reactive oxygen species production	No changes	Increased
Mitochondria hyperpolarization	Yes	Yes
Cell proliferation	No changes	No changes
Cell cycle	No changes	No changes
Expression of activation markers	No changes	No changes

Characterization of the Gal-1-mediated Apoptotic Pathway—Apoptosis is generally associated, as a late event, with the loss of MMP, the release of apoptogenic factors, *e.g.* apoptosis-inducing factor, endo G, and Cyt *c* and the consequent activation of caspase-9, which triggers the execution of cell death (17).

To gain insight the intracellular signaling pathways triggered by Gal-1, we performed a parallel analysis of caspase activity in the presence of the pan-caspase inhibitor ZVAD. Results clearly indicated that Gal-1 treatment induced a time-dependent activation of caspase-8 (Fas-associated caspase, Fig. 7*B*), caspase-9 (mitochondria-associated caspase, Fig. 7*C*), and the executioner caspase-3 (Fig. 7*D*). In particular, after 6 h of Gal-1 treatment, only caspase-8 (Fig. 7*B*), but not caspases-9 (Fig. 7*C*) or -3 (Fig. 7*D*) was activated. Accordingly, at this time, no release of Cyt *c* was observed (data not shown). However, prolonging the exposure to Gal-1 resulted in a time-dependent activation of caspases-9 and -3 (Fig. 7, *C* and *D*).

Considering the role of ceramide as a second messenger in

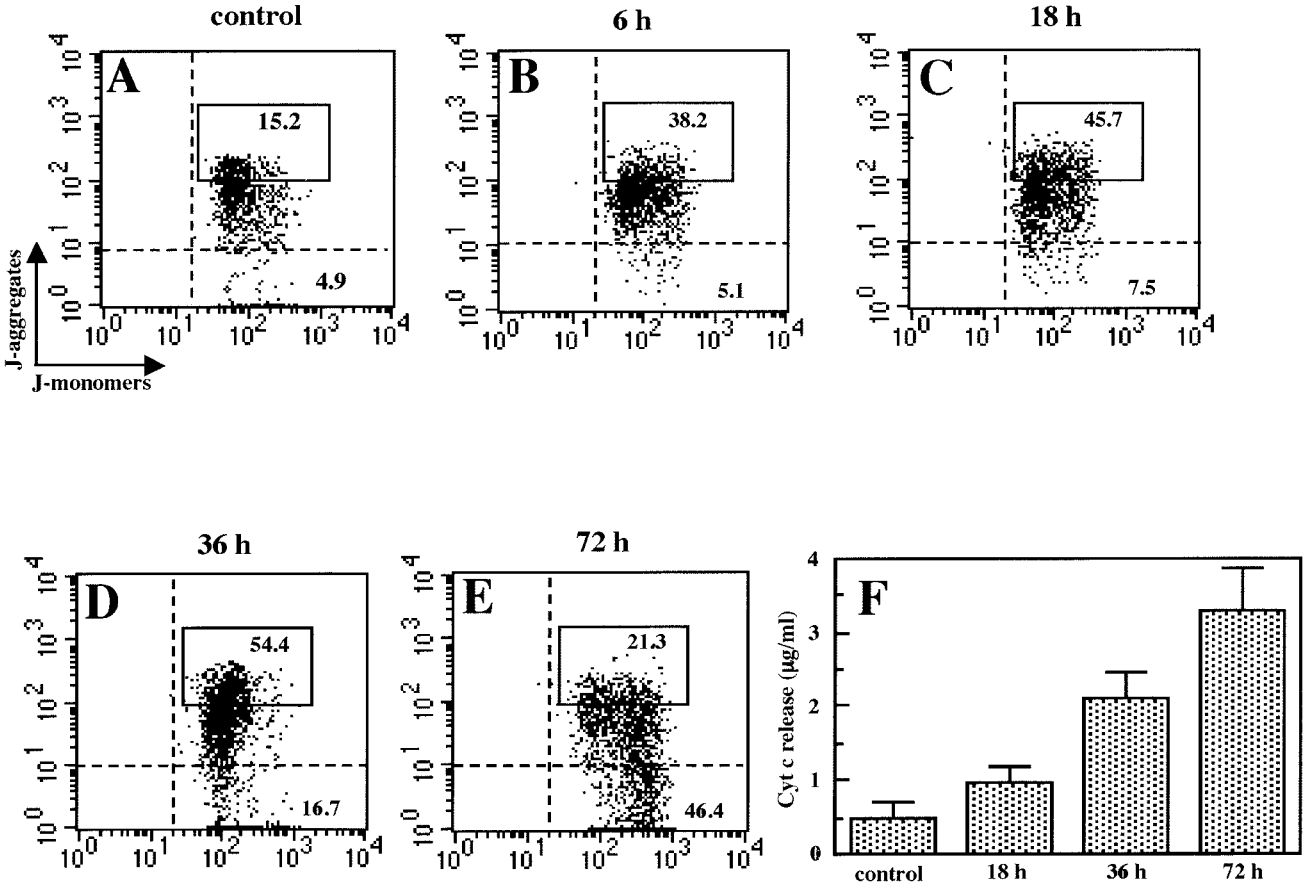

FIG. 6. **Time course analysis of the modulation of MMP and Cyt *c* release by Gal-1.** MMP were assessed by flow cytometry in resting T lymphocytes incubated in the absence (*A*) or presence of Gal-1 for 6 (*B*), 18 (*C*), 36 (*D*), and 72 h (*E*) and then stained with JC-1 (*A–E*). In the *boxed areas* the percentage of cells with high MMP are reported; *numbers* in the *lower right quadrants* indicate the percentage of cells with depolarized mitochondria. *F*, evaluation of Cyt *c* released from resting T lymphocytes. Note the dose-dependent effect of Gal-1.

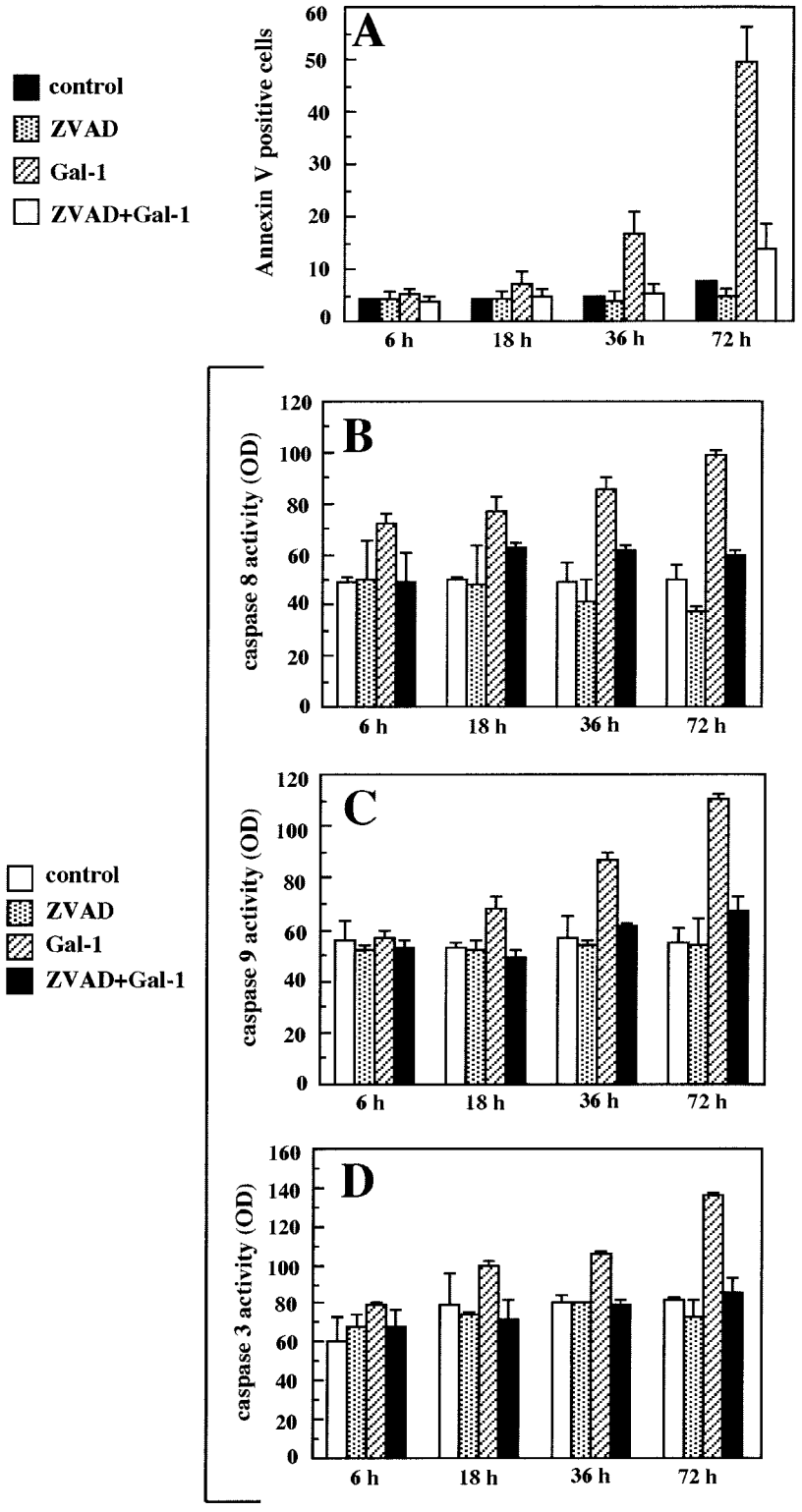

FIG. 7. **Characterization of the Gal-1-mediated apoptotic pathway: involvement of caspases.** *A*, cell death was examined by flow cytometry after annexin V staining of Gal-1-treated or untreated cells in the absence or presence of the pan-caspase inhibitor ZVAD. Activation state of caspase-8 (*B*), caspase-9 (*C*), and caspase-3 (*D*) in Gal-1-treated or untreated lymphocytes in the presence or absence of the pan-caspase inhibitor ZVAD is shown. As expected, ZVAD significantly ($p < 0.01$) prevented either apoptosis (*A*) or caspase-8 (*B*), caspase-9 (*C*), and caspase-3 (*D*) activation induced by Gal-1.

CD95-mediated apoptosis (33) and the potential role of this intracellular mediator in T cell death induced by certain galectins (34), FB_1 and Mon were used as specific inhibitors of the ceramide signaling pathway. Results obtained clearly showed that the administration of FB_1 and Mon was able to significantly prevent apoptosis induced by exposure to Gal-1 (Fig. 8, *D versus C*; $p < 0.01$). In particular, annexin V binding was decreased significantly (~60%) in resting T cells preexposed to ceramide inhibitors 1 h before the addition of Gal-1 (Fig. 8*D*). Accordingly, a significant inhibition of apoptosis-associated MMP loss was also observed (data not shown). Spectrophotometric analysis of the activation state of caspases-8, -9, and -3 also confirmed these data (Fig. 8*E*), the absorbance values obtained after Gal-1 exposure being significantly higher than those found in T lymphocytes pretreated with a mixture of FB_1 and Mon before the addition of Gal-1 ($p < 0.01$).

Effects of Gal-1 on Mitochondrial Coalescence, Budding, and Fission—On the basis of recent data describing a role for mitochondrial compartment "remodeling" in apoptotic cell death (20, 35), a specific set of experiments was performed aimed at

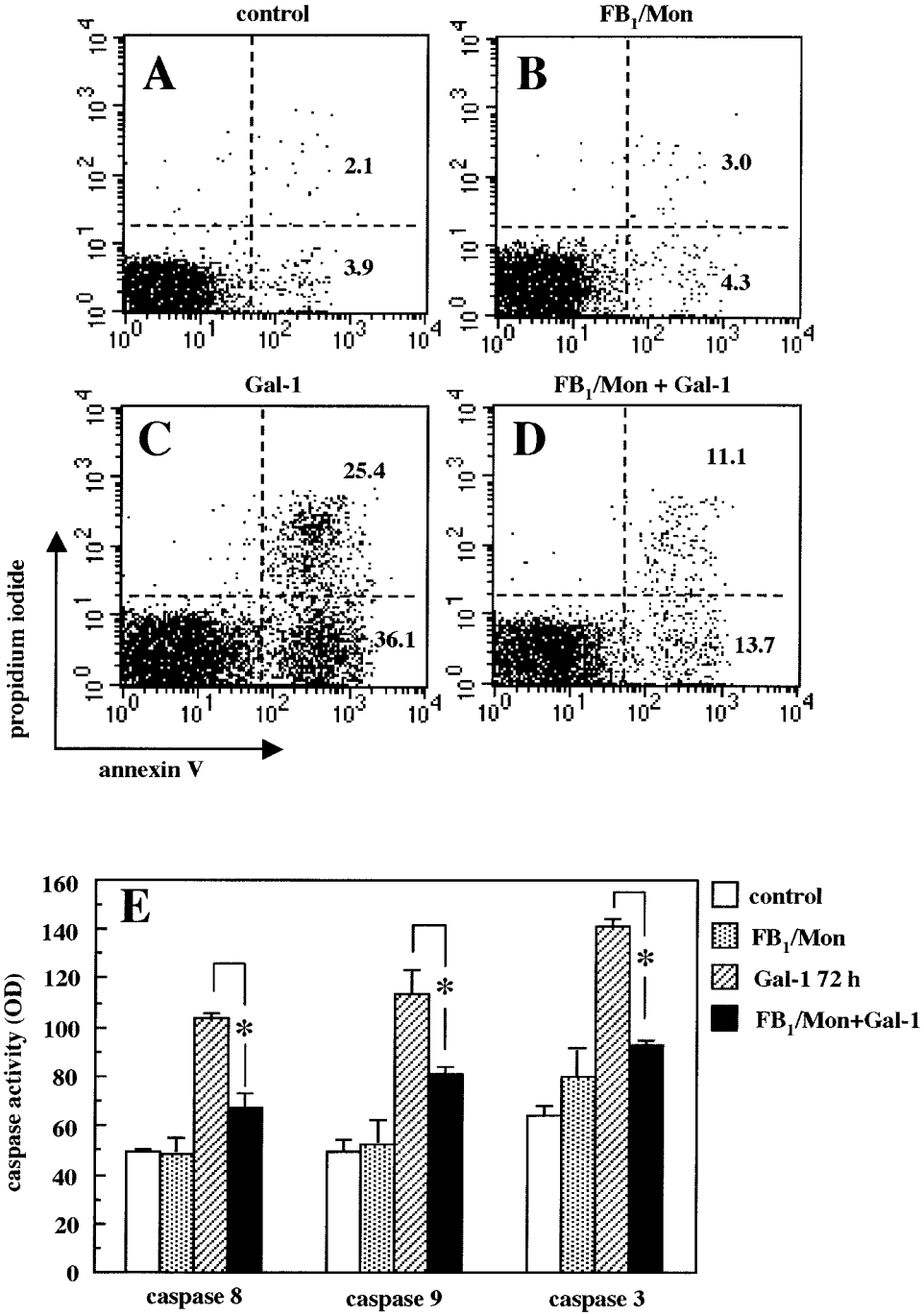

FIG. 8. **Role of the ceramide pathway in Gal-1-induced cell death.** Analysis of cell death after double staining with annexin V-FITC/PI. *A*, control cells; *B*, cells treated with a combination of FB_1 and Mon (inhibitors of the ceramide pathway); *C*, cells exposed to Gal-1 alone or *D*, in the presence of a FB_1/Mon combination. *Numbers* in the *upper* and *lower right quadrants* indicate the percentages of annexin V/PI double positive and annexin V single positive cells, respectively. *E*, spectrophotometric analysis of caspases-8, -9, and -3 activation under the conditions described above. *Asterisks* (*) represent $p < 0.01$.

analyzing ultrastructural features of mitochondria in Gal-1-treated resting cells and the behavior of key molecules involved in mitochondrial changes occurring in the early stages of apoptosis, *i.e.* h-Fis and DRP-1 (20, 35, 36). Our observations are summarized in Figs. 9–12. The sequence of events occurring in mitochondria after Gal-1 exposure were the following: (i) mitochondria, scattered throughout the cell cytoplasm in control untreated resting T lymphocytes (Fig. 9*A*), underwent redistribution at one pole of the cells after Gal-1 treatment (Fig. 9*B*). Next, (ii) a massive coalescence and clustering of the mitochondria was observed (Fig. 9*C*). Morphometric analyses carried out by TEM clearly demonstrated a significant increase of cells with clustered and marginalized mitochondria after Gal-1 treatment (Fig. 9*D*). Furthermore, in light of the results shown in Fig. 5, we evaluated the correlation between the percentages of cells displaying mitochondria with increased $\Delta\psi$ and cells with "marginalized" mitochondria. This analysis clearly indicated a statistically significant correlation ($r = 0.8979$; $p < 0.001$) between these two events. Moreover, we observed electrondense mitochondrial membranes budding from the mitochondrial "body" (Fig. 9*E*), which finally formed small pedunculated and whorled membrane structures (Fig. 9, *F* and *G*). In

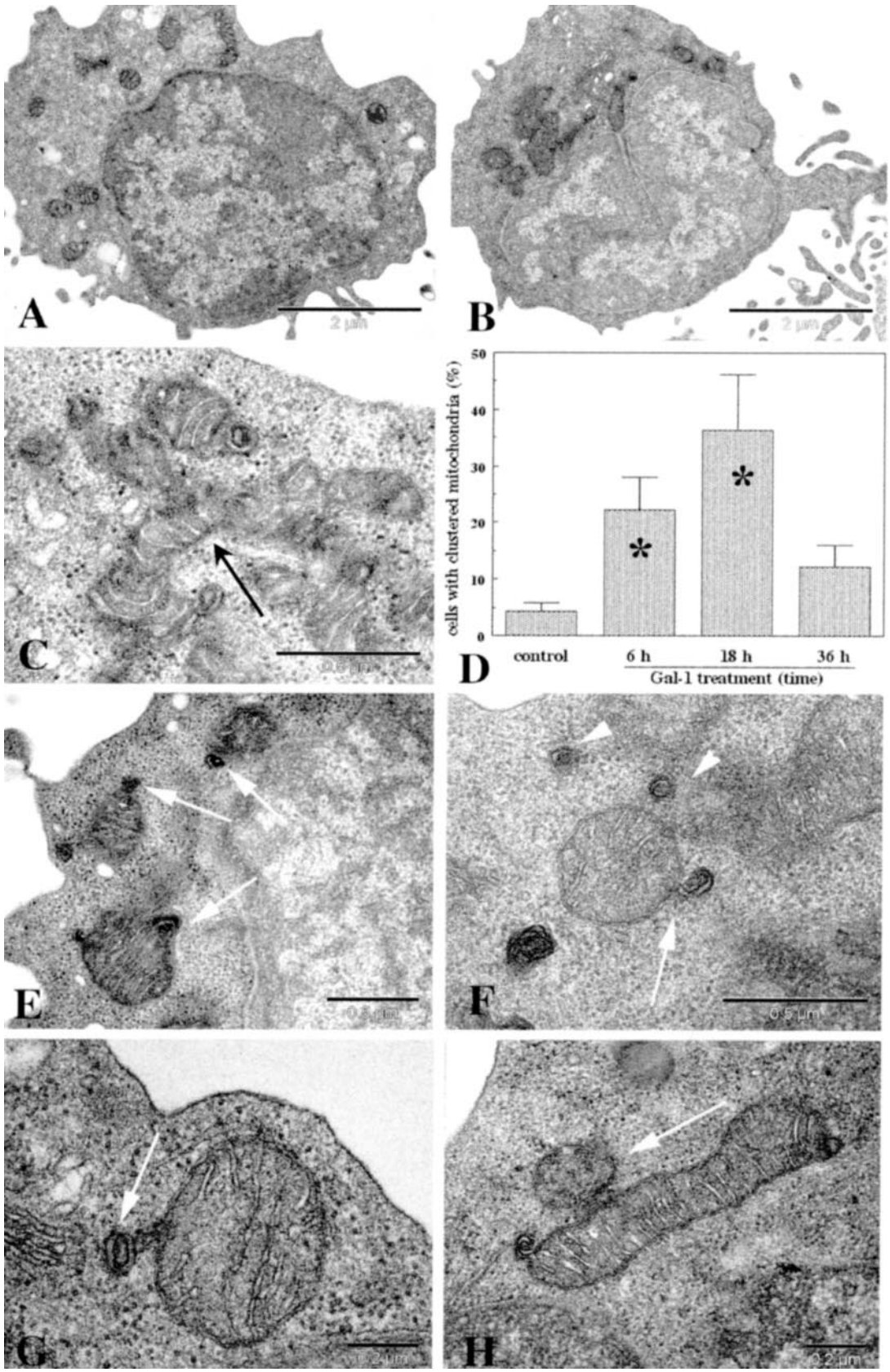

FIG. 9. **Ultrastructural analysis of resting T lymphocytes treated with Gal-1.** *A*, randomly distributed mitochondria were detectable in control cell cytoplasm. *B*, after exposure to Gal-1 for 18 h, mitochondria appeared clustered at one pole of the cell, undergoing coalescence (*C*, *arrow*). *D*, quantitative morphometric analyses revealed that the percentage of cells displaying mitochondrial clustering at one pole of the cell was increased significantly after 6 and 18 h of Gal-1 treatment. *Asterisks* (*) indicate a significant ($p < 0.01$) difference *versus* control untreated samples. Alterations of mitochondria occurring at early stages of apoptosis in Gal-1-treated resting T lymphocytes are shown in *E–H*. After an 18-h Gal-1 treatment, mitochondrial membrane budding structures were visible as small electron dense "blebs" (*E*, *arrows*). After a 36-h treatment, pedunculated membranous structures (*F* and *G*, *arrows*), sometimes whorled and detached from the organelle surface (*F*, *arrowheads*), were detected. Budding structures could also result in the formation of a sort of "newborn organelle" (*H*, *arrow*).

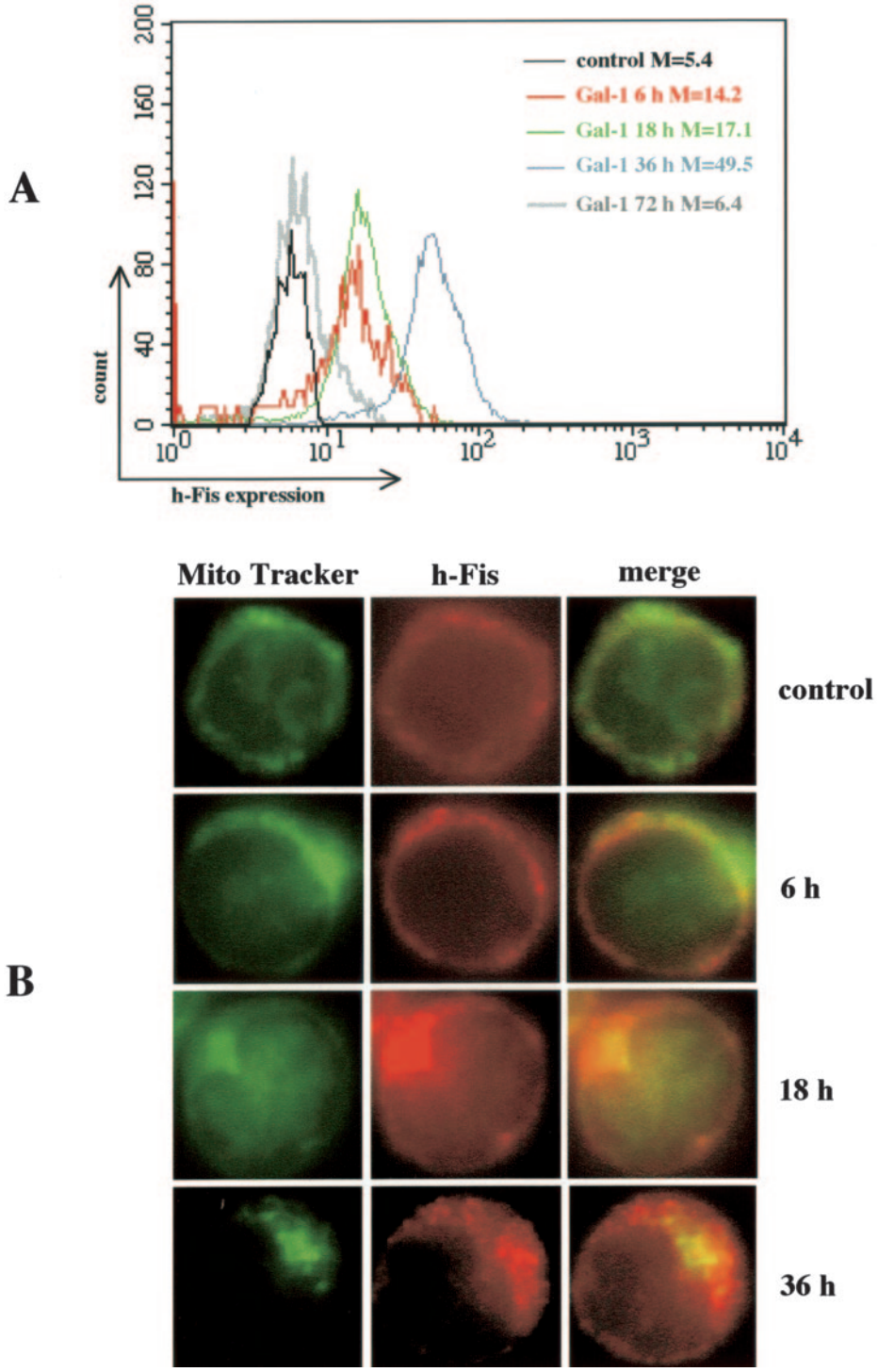

FIG. 10. **Evaluation of h-Fis expression and subcellular distribution in resting T lymphocytes.** *A*, quantitative flow cytometry analysis of h-Fis protein expression in T lymphocytes treated with Gal-1 for 6, 18, 36, and 72 h. Statistical analyses (Kolmogorov-Smirnov test) indicated a significantly ($p < 0.01$) increased expression of h-Fis. However, after a 72-h Gal-1 treatment, values detected were similar to those found in control samples ($p > 0.05$). *Numbers* reported in *A* indicate the median values of fluorescence intensity histograms obtained in T lymphocytes from a representative HD. *B*, intracytoplasmic localization of h-Fis obtained by IVM technique after double staining of Gal-1-treated T lymphocytes with a Mito Tracker Green probe (to detect mitochondria) and TRICT-conjugated mAb to h-Fis (*red* fluorescence). Fluorescence micrographs show that h-Fis is localized at one pole of T cells 18 or 36 h after Gal-1 treatment and is colocalized with mitochondria as demonstrated by merged pictures in the *right column*. Results obtained from a representative of eight HDs are reported.

some cases, these structures appeared detached from the mitochondrial body (Fig. 9*F*). These changes resulted in the formation of a small organelle with typical features of mitochondria (Fig. 9*H*). Notably, these changes were observed neither in control resting T cells nor after exposure to anti-Fas mAb.

Considering these observations, we next investigated the participation in this process of key molecules (h-Fis and DRP-1), which have been associated with morphogenetic changes occurring in mitochondria of dying cells. Both quantitative (by flow cytometry) and qualitative (by static cytometry) analyses were performed. Early after Gal-1 exposure (from 6 to 36 h), we found a time-dependent increase in h-Fis expression (Fig. 10*A*). This overexpression was, however, transient, and after 72 h h-Fis expression dropped down to lower "basal" levels. Parallel analyses carried out by IVM (Fig. 10*B*) showed a redistribution of this molecule in accordance with mitochondrial marginalization and coalescence as revealed by TEM analyses (Fig. 9*B*). More importantly, h-Fis appeared to be colocalized with polarized mitochondria (Fig. 10*B*). This observation was suggested by overlapping of green fluorescence (mitochondrial labeling) and red fluorescence (h-Fis), resulting in yellow staining in the merged pictures (see *right column* in Fig. 10*B*). Parallel analysis was also carried out to evaluate DRP-1 quantitative expression and intracellular localization (Fig. 11). Differently from h-Fis, no significant quantitative changes in DRP-1 expression were detected in Gal-1-treated cells with respect to control cells (Fig. 11*A*). By contrast, a well evident redistribution of DRP-1 molecule was detected in Gal-1-exposed resting T

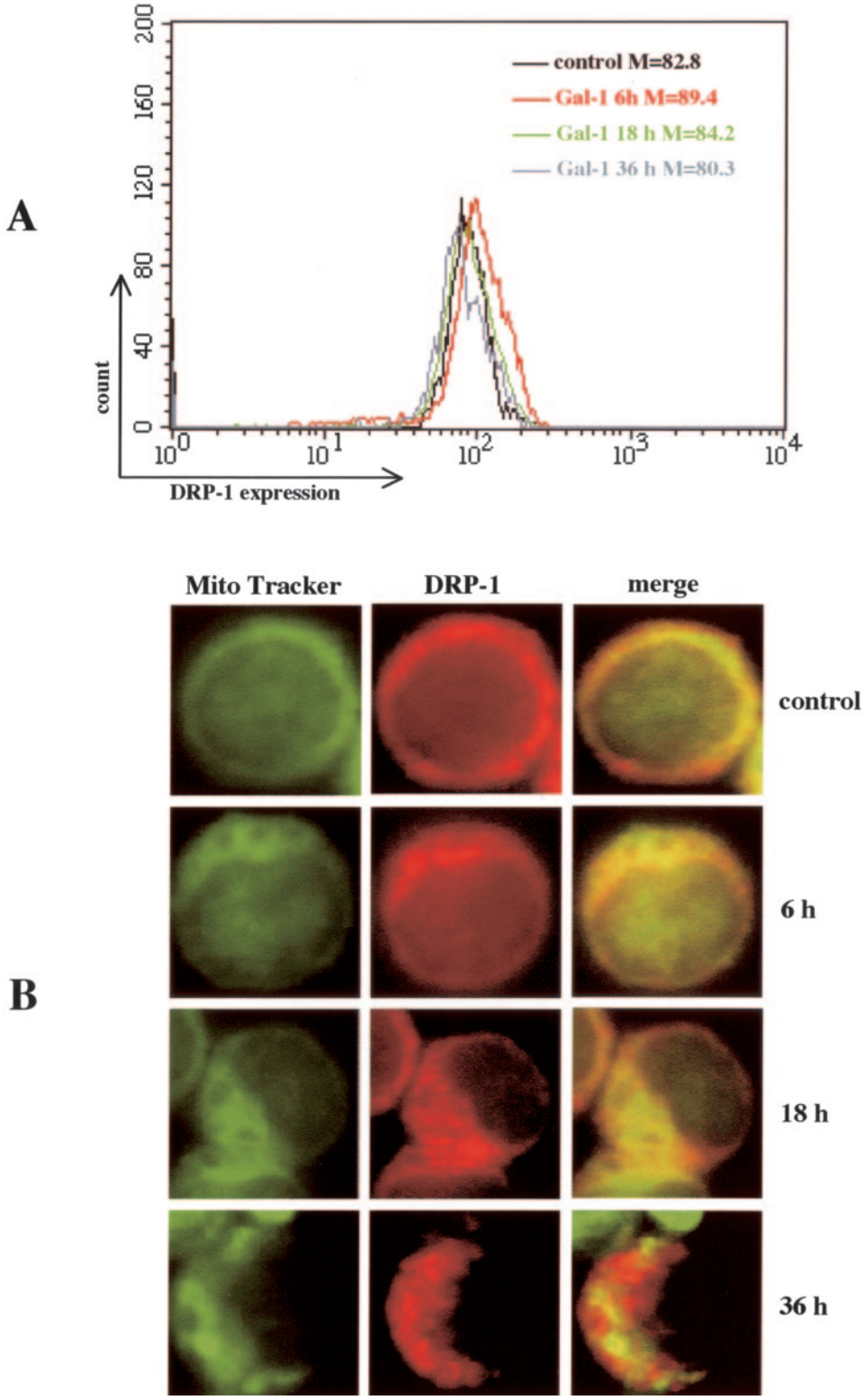

FIG. 11. **Evaluation of DRP-1 expression and localization in Gal-1-treated resting T lymphocytes.** Quantitative (*A*) and qualitative (*B*) analyses were carried out by flow cytometry and static IVM cytometry. *A*, no significant increase of DRP-1 expression ($p > 0.05$ by Kolmogorov-Smirnov test) was detected after Gal-1 treatment. Conversely, fluorescence micrographs (*B*) clearly indicated that mitochondria (revealed by Mito Tracker Green staining) and DRP-1 protein (detected by TRICT-conjugated mAb, in *red*) colocalize in untreated T lymphocytes (*first row*) as well as after a 6-h (*second row*) or 18-h (*third row*) Gal-1 exposure. After 36 h (*fourth row*), only a partial colocalization was detectable. Furthermore, both DRP-1 and mitochondria appeared distributed randomly in untreated T lymphocytes (*first row*) and marginalized after Gal-1 exposure (note the merged pictures on the *right*). The scattered positivity detectable after 36 h (*fourth row*) is suggestive of mitochondrial budding (compare with Fig. 9). Results obtained from a representative of eight HDs are shown.

lymphocytes by IVM analyses (Fig. 11*B*). In particular, starting from 6 h of Gal-1 treatment (*second row*), DRP-1 (*red* fluorescence) appeared to be organized as small spots, which colocalized to mitochondria (*green* fluorescence) resulting in the *yellow* staining visible in the merged pictures.

To deep inside the mechanisms involved in the mitochondrial

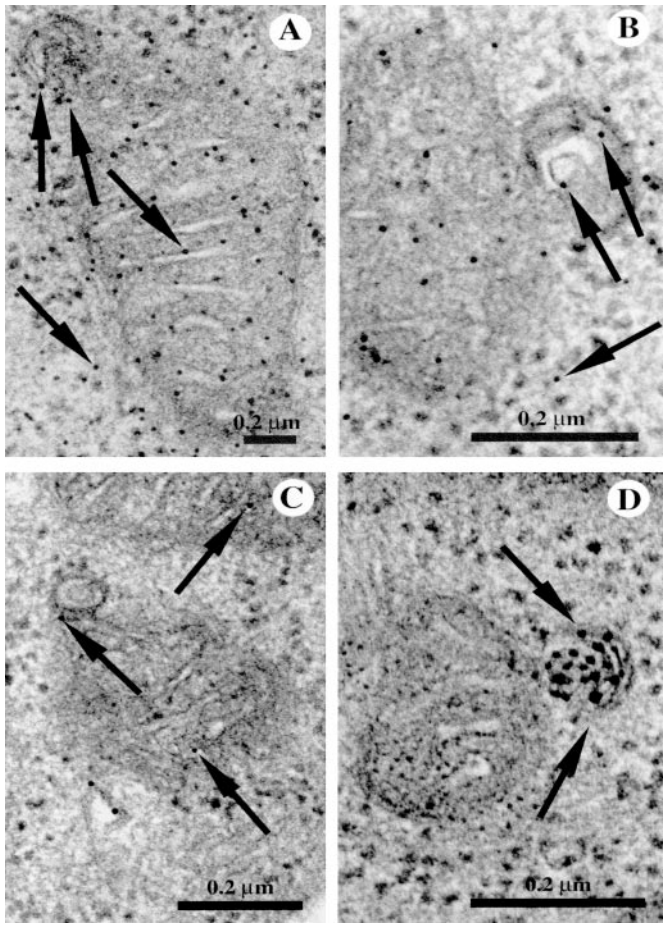

FIG. 12. **Immunogold labeling of mitochondrial fission-related molecules in Gal-1-treated resting T cells.** The analysis of the distribution of 10 nm gold particles revealed that after Gal-1 treatment, the apoptogenic factors endo G (*A*) and Cyt *c* (*B*) are detectable either on mitochondrial membranes, including the budding regions, or in the cell cytoplasm (*arrows*). Immunogold labeling also revealed the presence of h-Fis molecules on the mitochondrial membranes, including the budding region (*C*, *arrows*). Conversely, DRP-1 appeared clustered in the budding region of mitochondria (*D*, *arrows*).

changes induced by Gal-1, we also analyzed the expression and localization of UCP-2, an important endogenous protein involved in mitochondrial homeostasis (37). However, in our experimental system, Gal-1 treatment did not induce any significant modification in the expression of UCP-2 in resting lymphocytes (median values of fluorescence intensity histograms obtained by flow cytometry: 121.9 ± 12.3 in control cells and 119.7 ± 13.5 in Gal-1-treated cells).

Finally, TEM analyses of two key mitochondria-associated molecules of importance in the apoptotic cascade, Cyt *c* and endo G, were carried out by means of immunogold labeling postembedding technique (Fig. 12, *A* and *B*). The aim of these analyses was to evaluate the possible selective presence of these molecules in the budding regions of mitochondria. We found the presence of endo G (Fig. 12*A*) and Cyt *c* (Fig. 12*B*) in the budding regions as well as in the mitochondrial body and the cell cytoplasm of Gal-1-treated cells. Conversely, immunogold analyses regarding the mitochondrial fission-associated molecules h-Fis (Fig. 12*C*) and DRP-1 (Fig. 12*D*), clearly showed a different behavior of these proteins. In fact, h-Fis appeared associated with mitochondria outer and inner membranes (Fig. 12*C*, *arrows* indicate 10-nm gold particles), whereas DRP-1 appeared clustered in the budding regions of mitochondria in Gal-1-treated cells (Fig. 12*D*).

DISCUSSION

It is well known that a wide variety of biological and chemical agents, including Gal-1, can induce apoptosis of activated T lymphocytes (1, 17, 18). However, resting T cells are generally resistant to apoptotic stimuli (16, 18), and the molecular basis of this resistance still remains to be elucidated. The role of phenotypic features of activated T cells, including the expression of surface activation markers, such as CD69, major histocompatibility complex class II or CD38, the increased expression of CD95/Fas, as well as changes in MMP (*i.e.* a hyperpolarization state) have been considered as potential mechanisms implicated in the generation of susceptibility to cell death (32, 38). In the present work we demonstrate that Gal-1 not only bolsters CD95/Fas-mediated cell death but also induces *per se* cell death of resting lymphocytes. The mechanisms potentially involved in this effect might include: (i) a direct interaction of Gal-1 with CD95/Fas receptors; (ii) the up-regulation of CD95/Fas cell surface expression in resting T cells; and (iii) changes of MMP, *i.e.* hyperpolarization, in resting T cells.

Regarding the first mechanism, we found that anti-Fas neutralizing antibodies (ZB4 clone) were able to inhibit Gal-1-induced cell death. Accordingly, the apoptotic cascade triggered by Gal-1 involved the activation of caspase-8. These results suggest that Gal-1 induces the typical type I cell death pathway. This apparently conflicts with recent literature data in which Gal-1 was shown to promote apoptosis in stabilized lymphoblastoid cell lines via a caspase-independent pathway (39) or to induce phosphatidylserine exposure without inducing cell apoptosis (40). However, this discrepancy might depend on the different Gal-1 concentrations we used and/or, more importantly, on different experimental systems considered (freshly isolated lymphocytes *versus* tumor cell lines). It is, in fact, well known that the metabolism of tumor cells, in particular lymphoblastoid cells, mainly anaerobic, significantly differs from that of freshly isolated lymphocytes. Accordingly, lymphoblastoid cell lines are not responsive to apoptosis-modulating drugs, *e.g.* to human immunodeficiency virus protease inhibitors, which are instead very effective both *in vivo* as well as *in vitro*, *i.e.* on freshly isolated lymphocytes (31). Hence, on the basis of the previously hypothesized immunoregulatory role exerted *in vivo* by Gal-1 (6, 14), the present study was focused on understanding the mechanisms involved in Gal-1-induced cell death in a physiological model system, *i.e.* freshly isolated human T cells. In fact, during the past few years Gal-1 has been shown to act as a negative immune regulator under physiopathological situations including autoimmunity (6, 8), cancer (14, 41, 42), and infection (42–44). The observations presented in this study provide a molecular basis for the immunoregulatory properties of this protein.

As regards resting T lymphocytes, important modifications of these cells seem to be induced by the administration of Gal-1, *e.g.* increased CD95/Fas expression and mitochondrial morphogenetic changes. No changes either in the expression of cell surface activation markers or in cell cycle progression and intracellular redox balance were detected. Hence, the ability of Gal-1 to induce significant apoptosis of resting cells seems to be associated with partial mimicking of activation-induced cell death, at least in terms of Gal-1-induced Fas overexpression and mitochondrial predisposition to apoptosis, *i.e.* increased MMP. A characteristic increase of $\Delta\psi$ (hyperpolarization) as well as changes in mitochondrial ionic homeostasis have in fact been detected in different cell types as earlier signs of increased apoptotic proneness (32, 45–47). In this context, our data indicate that the increase in MMP generated by Gal-1 might represent a critical event in bolstering cell death. A parallel event

related to the influence of Gal-1 on mitochondrial homeostasis is represented by the redistribution of these organelles that migrate to one pole of the cells. This effect was followed by a massive mitochondrial coalescence, the formation of budding regions on mitochondria, and, apparently, by fission processes, late mitochondrial alterations known to be associated with cell death execution and $\Delta\psi$ loss (45, 46, 48).

The role of mitochondrial fission and fusion processes has recently been taken into consideration in the context of programmed cell death (20). It has been hypothesized that an imbalance in favor of the mitochondrial fission process may occur in cells undergoing apoptosis, although the fusion process was reported to be associated with cell senescence and survival. It has also been suggested that dissipation of MMP might shift mitochondria toward fragmentation (36), thus contributing to apoptotic cell death. Fusion and fission processes are instructed by a series of molecules, including DRP-1 and h-Fis (20). The first is a GTPase from the dynamin family, which was hypothesized to be localized mainly to the outer mitochondrial membrane. The second was described as an integral protein of the outer mitochondrial membrane able to recruit DRP-1 to the fission foci participating in the membrane scission events. However, little is known to date about the precise role of these two molecules in physiological systems of programmed cell death (20, 35). For instance, some data have been obtained by studying dominant-negative mutants of DRP-1. In this experimental system, the mitochondrial fission process was blocked and resulted in the inhibition of apoptosis (20). In the same vein, it has been suggested that DRP-1 could modulate tumor cell susceptibility to cell death and contribute to the execution of the apoptotic cascade (20, 35). In our experimental system, *i.e.* freshly isolated human resting T lymphocytes, the induction of mitochondrial remodeling appeared to be associated with a transient but significant increase of h-Fis expression. By contrast, Gal-1 treatment did not induce any quantitative change in DRP-1 expression. However, a redistribution of DRP-1, which was concentrated in the budding regions of mitochondria, was clearly observed. This is the first demonstration that DRP-1 could effectively be recruited to participate in the mitochondrial fission events. Furthermore, in Gal-1-induced cell death of human T lymphocytes mitochondrial morphogenetic changes precede other signs of apoptosis, *e.g.* nuclear chromatin condensation and fragmentation. This seems thus to represent a suitable physiological model system to study the role of mitochondrial remodeling occurring during cell death.

Members of the sphingomyelin pathway have a profound influence on the apoptotic cascade, including mitochondrial changes (49). It has also been hypothesized that ceramide tends to self-aggregate, and its asymmetrical formation in the membrane, *e.g.* in lipid rafts, may induce negative membrane curvature, which precedes budding and vesiculation (49). On the basis of our results, we cannot rule out the possibility that the increased glycosyltransferase activity caused by Gal-1 treatment might lead to the formation of glycosphingolipid species as second messengers modulating mitochondrial membrane structure and dynamics. In light of recent literature data, it can also be hypothesized that another member of the galectin family, Gal-3, may also protect normal, nontransformed lymphocytes from Gal-1-induced cell death. Gal-3 has in fact been shown to protect against Gal-1-induced cell death (39), to prevent mitochondrial damage (50), and to promote resistance to C2-ceramide-mediated apoptosis (34). Finally, lipid rafts are mainly composed of sphingolipids and have been demonstrated to be involved in mitochondria-dependent Fas-induced apoptosis (51) as well as in subcellular activities exerted by galectins, including Gal-1 (4, 50). Hence, on the basis of our findings using specific inhibitors of the ceramide pathway, which are also able to block mitochondrial fission process, we propose that Gal-1 could trigger morphogenetic changes of the mitochondria via a ceramide-mediated pathway. Recent studies also indicate that other galectins, such as Gal-2 (52), Gal-3 (34), and Gal-9 (53), can promote T cell apoptosis with distinct profiles of caspase activation and different intracellular signaling events.

In conclusion, our results, obtained by using nonimmortalized and nonengineered freshly isolated T lymphocytes, indicate that Gal-1 can be an excellent model system to analyze the intracellular events and the role of the morphogenetic changes of mitochondria in the apoptotic cascade. Our observations also suggest that this endogenous lectin might play a relevant role by bolstering physiological Fas-mediated apoptosis in immune cells. Therefore, Gal-1-mediated death of T lymphocytes may contribute to immune cell homeostasis and to a successful escape of tumors from immune surveillance by hindering T cell-mediated immune reactivity.

REFERENCES

1. Rabinovich, G. A., Baum, L. G., Tinari, N., Paganelli, R., Natoli, C., Liu, F. T., and Iacobelli, S. (2002) *Trends Immunol.* **23,** 313–320
2. Liu, F. T. (2000) *Clin. Immunol.* **97,** 79–88
3. Rabinovich, G. A., Rubinstein, N., and Toscano, M. A. (2002) *Biochim. Biophys. Acta* **1572,** 274–284
4. Chung, C. D., Patel, V. P., Moran, M., Lewis, L. A., and Miceli, M. C. (2000) *J. Immunol.* **165,** 3722–3729
5. Rabinovich, G. A., Ramhorst, R. E., Rubinstein, N., Corigliano, A., Daroqui, M. C., Kier-Joffe, E. B., and Fainboim, L. (2002) *Cell Death Differ.* **9,** 661–670
6. Rabinovich, G. A., Daly, G., Dreja, H., Tailor, H., Riera, C. M., Hirabayashi, J., and Chernajovsky, Y. (1999) *J. Exp. Med.* **190,** 385–398
7. Rabinovich, G. A, Ariel, A., Hershkoviz, R., Hirabayashi, J., Kasai, K. I., and Lider, O. (1999) *Immunology* **97,** 100–106
8. Santucci, L., Fiorucci, S., Rubinstein, N., Mencarelli, A., Palazzetti, B., Federici, B., Rabinovich, G. A., and Morelli, A. (2003) *Gastroenterology* **124,** 1381–1384
9. Perillo, N. L., Pace, K. E., Seilhamer, J. J., and Baum, L. G. (1995) *Nature* **378,** 736–739
10. Rabinovich, G. A., Iglesias, M. M., Modesti, N. M., Castagna, L. F., Wolfenstein-Todel, C., Riera, C. M., and Sotomayor, C. E. (1998) *J. Immunol.* **160,** 4831–4840
11. He, J., and Baum, L. G. (2004) *J. Biol. Chem.* **279,** 4705–4712
12. Galvan, M., Tsuboi, S., Fukuda, M., and Baum, L. G. (2000) *J. Biol. Chem.* **275,** 16730–16737
13. Amano, M., Galvan, M., He, J., and Baum, L. G. (2003) *J. Biol. Chem.* **278,** 7469–7475
14. Rubinstein, N., Alvarez, M., Zwirner, N. W., Toscano, M. A., Ilarregui, J. M., Bravo, A., Mordoh, J., Fainboim, L., Podhajcer, O. L., and Rabinovich, G. A. (2004) *Cancer Cell* **5,** 241–251
15. Roberts, A. I., Devadas, S., Zhang, X., Zhang, L., Keegan, A., Greeneltch, K., Solomon, J., Wei, L., Das, J., Sun, E., Liu, C., Yuan, Z., Zhou, J. N., and Shi, Y. (2003) *Immunol. Res.* **28,** 285–293
16. Baumann, S., Krueger, A., Kirchhoff, S., and Krammer, P. H. (2002) *Curr. Mol. Med.* **2,** 257–272
17. Green, D. R., Droin, N., and Pinkoski, M. (2003) *Immunol. Rev.* **193,** 70–81
18. Lenardo, M. J. (2003) *Immunol. Res.* **27,** 387–398
19. Slee, E. A., Adrain, C., and Martin, S. J. (1999) *Cell Death Differ.* **6,** 1067–1074
20. Karbowski, M., and Youle, R. J. (2003) *Cell Death Differ.* **10,** 870–880
21. Zamzami, N., and Kroemer, G. (2001) *Nat. Rev. Mol. Cell. Biol.* **2,** 67–71
22. Hirabayashi, J., Ayaki, H., Soma, G., and Kasai, K. (1989) *FEBS Lett.* **250,** 161–165
23. Merril, A. H., Liotta, D. C., and Riley, R. (1996) *Trends Cell Biol.* **6,** 218–223
24. Mendez, A. J. (1995) *J. Biol. Chem.* **270,** 5891–5900
25. Conti, L., Rainaldi, G., Matarrese, P., Varano, B., Rivabene, R., Columba, S., Sato, A., Belardelli, F., Malorni, W., and Gessani, S. (1998) *J. Exp. Med.* **187,** 403–413
26. Cossarizza, A., Franceschi, C., Monti, D., Salvioli, S., Bellesia, E., Rivabene, R., Biondo, L., Rainaldi, G., Tinari, A., and Malorni, W. (1995) *Exp. Cell Res.* **220,** 232–240
27. Casciola-Rosen, L., Nicholson, D. W., Chong, T., Rowan, K. R., Thornberry, N. A., Miller, D. K., and Rosen, A. (1996) *J. Exp. Med.* **183,** 1957–1964
28. Parlato, S., Giammarioli, A. M., Logozzi, M., Lozupone, F., Matarrese, P., Luciani, F., Falchi, M., Malorni, W., and Fais, S. (2000) *EMBO J.* **19,** 5123–5134
29. Hildeman, D. A. (2004) *Free Rad. Biol. Med.* **36,** 1496–1504
30. Banki, K., Hutter, E., Gonchoroff, N. J., and Perl, A. (1999) *J. Immunol.* **162,** 1466–1479
31. Matarrese, P., Gambardella, L., Cassone, A., Vella, S., Cauda, R., and Malorni, W. (2003) *J. Immunol.* **170,** 6006–6015
32. Matarrese, P., Cauda, R., and Malorni, W. (2003) *Cell Death Differ.* **10,** 609–611
33. Cuvillier, O., Edsall, L., and Spiegel, S. (2000) *J. Biol. Chem.* **275,** 15691–15700

34. Fukumori, T., Takenaka, Y., Oka, N., Yoshii, T., Hogan, V., Inohara, H., Kanayama, H. O., Kim, H. R., and Raz, A. (2004) *Cancer Res.* **64,** 3376–3379
35. Bossy-Wetzel, E., Barsoum, M. J., Godzik, A., Schwarzenbacher, R., and Lipton, S. A. (2003) *Curr. Opin. Cell Biol.* **15,** 706–716
36. Ishihara, N., Jofuku, A., Eura, Y., and Mihara, K. (2003) *Biochem. Biophys. Res. Commun.* **301,** 891–898
37. Mattson, M. P., and Liu, D. (2003) *Biochem. Biophys. Res. Commun.* **304,** 539–549
38. Krueger, A., Fas, S. C., Baumann, S., and Krammer, P. H. (2003) *Immunol. Rev.* **193,** 58–69
39. Hahn, H. P., Pang, M., He, J., Hernandez, J. D., Yang, R.-Y., Li, L. Y., Wang, X., Liu, F.-T., and Baum, L. G. (2004) *Cell Death Differ.* **11,** 1277–1286
40. Dias-Baruffi, M., Zhu, H., Cho, M., Karmakar, S., McEver, R. P., and Cummings, R. D. (2003) *J. Biol. Chem.* **278,** 41282–41293
41. Rappl, G., Abken, H., Muche, J. M., Sterry, W., Tilgen, W., Andre, S., Kaltner, H., Ugurel, S., Gabius, H. J., and Reinhold, U. (2002) *Leukemia* **16,** 840–845
42. Roberts, A. A., Amano, M., Feltren, C., Galvan, M., Sulur, G., Pinter-Brown, L., Dobbeling, U., Burg, G., Said, J., and Baum, L. G. (2003) *Mod. Pathol.* **16,** 543–551
43. Zúñiga, E. I., Gruppi, A., Hirabayashi, J., Kasai, K. I., and Rabinovich, G. A. (2001) *Infect. Immun.* **69,** 6804–6812
44. Lanteri, M., Giordanengo, V., Hiraoka, N., Fuzibet, J. G., Auberger, P., Fukuda, M., Baum, L. G., and Lefebvre, J. C. (2003) *Glycobiology* **13,** 909–918
45. Giovannini, C., Matarrese, P., Scazzocchio, B., Sanchez, M., Masella, R., and Malorni, W. (2002) *FEBS Lett.* **523,** 200–206
46. Nagy, G., Koncz, A., and Perl, A. (2003) *J. Immunol.* **171,** 5188–5197
47. Perl, A., Gergely, P., Jr., Nagy, G., Koncz, A., and Banki, K. (2004) *Trends Immunol.* **25,** 360–367
48. Green, D. R., and Kroemer, G. (2004) *Science* **305,** 626–629
49. van Blitterswijk, W. J., van der Luit, A. H., Veldman, R. J., Verheij, M., and Borst, J. (2003) *Biochem. J.* **369,** 199–211
50. Matarrese, P., Tinari, N., Semeraro, M. L., Natoli, C., Iacobelli, S., and Malorni, W. (2000) *FEBS Lett.* **473,** 311–315
51. Prior, I. A., Muncke, C., Parton, R. G., and Hancock, J. F. (2003) *J. Cell Biol.* **160,** 165–170
52. Sturm, A., Lensch, M., Andre, S., Kaltner, H., Wiedenmann, B., Rosewicz, S., Dignass, A. U., and Gabius, H. J. (2004) *J. Immunol.* **173,** 3825–3837
53. Kashio, Y., Nakamura, K., Abedin, M. J., Seki, M., Nishi, N., Yoshida, N., Nakamura, T., and Hirashima, M. (2003) *J. Immunol.* **170,** 3631–3636